(accepted)

A Tale of Tails: Dark Matter Interpretations of the Fermi GeV Excess in Light of Background Model Systematics

Francesca Calore,[1,*] Ilias Cholis,[2,†] Christopher McCabe,[1,‡] and Christoph Weniger[1,§]

[1] *GRAPPA, University of Amsterdam, Science Park 904, 1098 XH Amsterdam, Netherlands*
[2] *Center for Particle Astrophysics, Fermi National Accelerator Laboratory, Batavia, IL, 60510, USA*

Several groups have identified an extended excess of gamma rays over the modeled foreground and background emissions towards the Galactic center (GC) based on observations with the *Fermi* Large Area Telescope. This excess emission is compatible in morphology and spectrum with a telltale sign from dark matter (DM) annihilation. Here, we present a critical reassessment of DM interpretations of the GC signal in light of the foreground and background uncertainties that some of us recently outlaid in Calore et al. 2014. We find that a much larger number of DM models fits the gamma-ray data than previously noted. In particular: (1) In the case of DM annihilation into $\bar{b}b$, we find that even large DM masses up to $m_\chi \simeq 74$ GeV are allowed at p-value > 0.05. (2) Surprisingly, annihilation into non-relativistic hh gives a good fit to the data. (3) The inverse Compton emission from $\mu^+\mu^-$ with $m_\chi \sim 60$–70 GeV can also account for the excess at higher latitudes, $|b| > 2^\circ$, both in its spectrum and morphology. We also present novel constraints on a large number of mixed annihilation channels, including cascade annihilation involving hidden sector mediators. Finally, we show that the current limits from dwarf spheroidal observations are not in tension with a DM interpretation when uncertainties on the DM halo profile are accounted for.

PACS numbers: 95.30.Cq,95.35+d,95.85.Pw,FERMILAB-PUB-14-477-A

I. INTRODUCTION

Shedding light onto the origin of Dark Matter (DM) is one of the biggest challenges of current particle physics and cosmology. The most appealing particle DM candidates are the so-called Weakly Interacting Massive Particles (WIMP) [1–3]. Among the different indirect messengers, gamma rays play a dominant role and they have often been defined as the *golden channel* for DM indirect detection (see Ref. [4] for an extensive review). The main challenge is to disentangle putative DM signals from the large astrophysical foregrounds and backgrounds that are generally expected to dominate the measured fluxes. The best example of a challenging target is the Galactic Center (GC), where on the one hand the DM signal is expected to be brighter than anywhere else on the sky [5, 6], but – given our poor knowledge of the conditions in the inner Galaxy – the astrophysical foreground and background (either from Galactic point sources or from diffuse emissions) is subject to very large uncertainties.

In this respect, it is not surprising for unmodeled gamma-ray contributions to be found towards the inner part of the Galaxy, above or below the expected standard astrophysical emission. Indeed, an extended excess in gamma rays at the GC was reported by different independent groups [7–16], using data from the *Fermi* Large Area Telescope (LAT), and dubbed "*Fermi* GeV excess" as it appears to peak at energies around 1–3 GeV. Intriguingly, the excess emission shows spectral and morphological properties consistent with signals expected from DM particles annihilating in the halo of the Milky Way. Recently, the existence of a GeV excess emission towards the GC above the modeled astrophysical foreground/background was also confirmed by the *Fermi*-LAT Collaboration [17]. This revitalizes the importance of understanding the origin of this excess.

Given that the Galactic diffuse emission is maximal along the Galactic disk and that a DM signal is expected to be approximately spherical, the preferable region to search for a DM annihilation signal in *Fermi*-LAT data is actually a region that, depending on the DM profile, extends between a few degrees and a few tens of degrees away from the GC, above and below the disk [18–23]. Indeed, different groups [15, 24, 25] extracted an excess with spectral properties similar to the GeV excess at the GC from the gamma-ray data at higher Galactic latitudes, up to about $|b| \sim 20^\circ$. The extension to higher latitudes is a critical test that the DM interpretation had to pass, and apparently has passed.

However, when talking about excesses, a rather central question is: *An excess above what?* The excess emission is defined above the astrophysical foregrounds and backgrounds, *i.e.* the Galactic diffuse emission, point sources and extended sources, modeled in the data analysis. Most previous studies of the *Fermi* GeV excess are based on a small number of fixed models for the Galactic diffuse emission. These models were built for the sole purpose of point source analyses and hence introduce uncontrollable systematics in the analysis of extended diffuse sources. In addition, since they are the result of fits to the data, they may falsely absorb part of the putative excess emission in some of their free components. This may in turn, lead to biased or overly constraining statements about the spectrum and morphology of the *Fermi*

* f.calore@uva.nl
† cholis@fnal.gov
‡ c.mccabe@uva.nl
§ c.weniger@uva.nl

GeV excess emission.

To remedy this situation, in Ref. [26] some of the present authors reassessed the spectral and morphological properties of the putative GeV excess emission from the inner Galaxy[1]. Relevant systematic uncertainties came from the modeling of the Galactic diffuse emission, *Fermi*-LAT detected point sources and the *Fermi* bubbles. The emission associated with the inner Galaxy was found to be larger than expected from standard Galactic diffuse emission models (where the distribution of the cosmic-ray (CR) sources peaks at kpc distances from the GC [27]). This "excess" is – by definition – an excess above Galactic diffuse emission models that lead to subdominant contribution from the inner kpc around the GC. It hence should be understood as a *characterization* of the dominant part of the emission from these central spatial regions, which is robust w.r.t. uncertainties in the emission from other parts along the line-of-sight. This emission features a spectrum that rises at energies below 1 GeV with a spectral index harder than two, peaks at 1–3 GeV, and has a high-energy tail that continues up to 100 GeV. The large uncertainties in the spectrum were estimated from a study of residuals along the Galactic disk. The observed emission was found to be consistent with the hypothesis of a uniform gamma-ray energy spectrum at 95% CL, with spherical symmetry around the GC and a radial extension of at least 1.5 kpc.

The proper treatment of systematic uncertainties has important consequences for the interpretation of the *Fermi* GeV excess: Although all studies find that the emission peaks around 1–3 GeV, the *low- and high-energy tails* of the spectrum are much more uncertain. As we will see below, this allows significant – previously ignored – freedom for DM models fitting the excess.

In what follows, we focus on the DM interpretations of the excess emission. We will therefore not further discuss potential astrophysical explanations, like the emission from an unresolved population of point-like sources concentrated in the very center of the Galaxy (see [28–31] for relevant discussions) or the injection of leptons and/or protons during a burst event at the GC some kilo-/mega-years ago [32, 33]. In particular, we will here entertain the possibility that *all* of the excess emission is coming from a single diffuse source. This obviously does not have to be the case, but it is a suggestive (and from the perspective of a particle physicist minimal) assumption, given the uniform spectral properties of the emission in different regions of the sky [26].

As for the DM interpretation, there is by now an extensive array of DM scenarios that both can explain the observed emission by DM annihilation while simultaneously being compatible with other direct, indirect and collider constraints [34–81]. The most relevant *indirect* constraints on DM models come from the non-observation of spectral features in the AMS-02 measurements of CR positrons [82, 83], and PAMELA observations of the CR anti-protons [84–89] (see however Ref. [90]).

Another important set of targets for indirect DM searches, which are, by comparison to the GC, more simple targets, are *dwarf spheroidal galaxies* (dSph). No gamma-ray emission has been detected so far from such objects, and strong constraints have been set on the DM annihilation signals [91–94]. These results are in general considered to be rather robust (see however Ref. [92]), and we will discuss in detail the impact of these limits on the DM interpretation of the *Fermi* GeV excess.

The goal of the present paper is three-fold: First, we will characterize, for the first time and in a coherent way, the impact of foreground model systematics as discussed in Ref. [26] on possible DM interpretations of the *Fermi* GeV excess, and show that a much larger number of DM models is viable than what was claimed before. Second, we will elaborate on the role of Inverse Compton Scattering (ICS) emission at higher latitudes in the case of leptonic channels. And third, we will discuss the impact of recent limits from dSphs on the DM interpretation of the *Fermi* GeV excess.

The paper is organized as follows: In Sec. II, we discuss the (non-)consistency of previous results for the intensity of the *Fermi* GeV excess at energies of 2 GeV, with emphasis on the higher-latitude *tail* of the emission. In Sec. III, we revise the main contributions to the gamma-ray sky coming from the CR interactions with the interstellar medium and we summarize the uncertainties affecting the modeling of the Galactic diffuse emission. We then describe how these uncertainties affect the low- and high-energy *tails* of the energy spectrum of the *Fermi* GeV excess. In Sec. IV, we discuss possible models for the DM interpretation of the *Fermi* GeV excess by analyzing different pure and mixed final states with and without inverse Compton emission. Last but not least, in Sec. V, we compare the findings about the *Fermi* GeV excess with the current constraints on the DM parameter space coming from the analysis of dwarf spheroidal galaxies, in light of observational constraints on the DM halo of the Milky Way. In Sec. VI we conclude.

II. THE "*FERMI* GEV EXCESS" AS A GENUINE FEATURE IN THE GAMMA-RAY SKY

In Fig. 1 we present a convenient comparison of the differential intensity of the *Fermi* GeV excess emission as derived by different groups, both for the GC in the inner few degrees, as well as the *higher-latitude tail* up to $\psi \sim 20^\circ$. We show the differential intensity at a reference energy of 2 GeV. At this energy the

[1] With *inner Galaxy* we refer to the region contained in few tens of degrees away from the GC and avoiding the very inner few degrees in latitude. In particular, in Ref. [26] the region considered is $|l| < 20^\circ$ and $2^\circ < |b| < 20^\circ$.

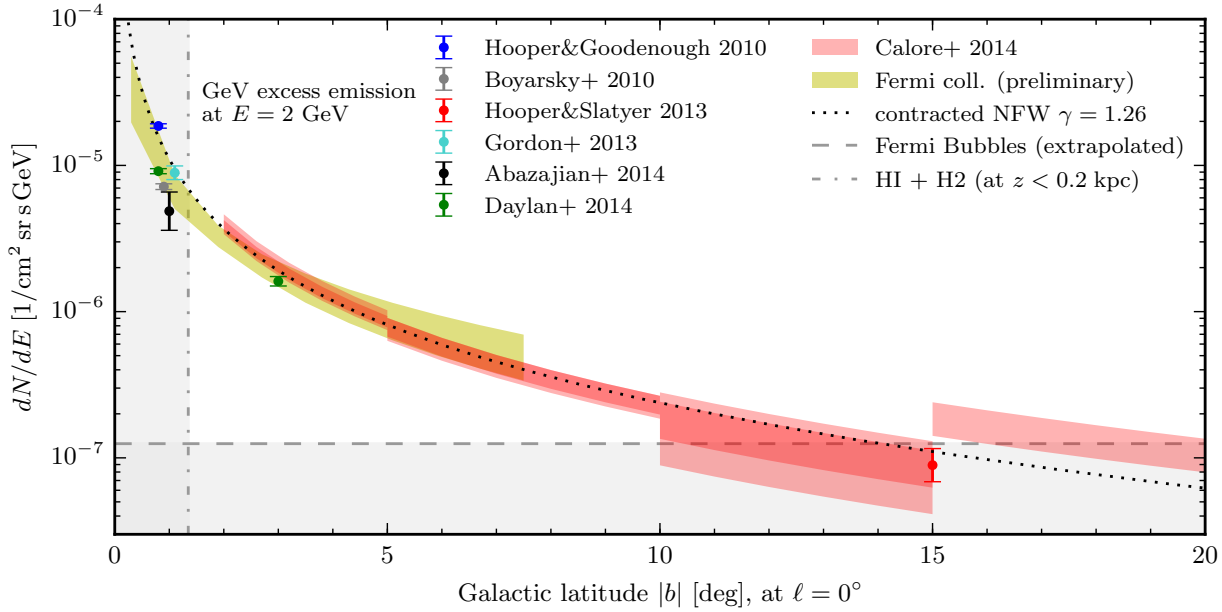

FIG. 1. Intensity of the *Fermi* GeV excess at 2 GeV as function of Galactic latitude (see text for details), compared with the expectations for a contracted NFW profile (*dotted line*). Error bars refer to statistical $\pm 1\sigma$ uncertainties, except for Refs. [13, 14] for which we take into account the quoted systematics coming from different astrophysical models. The result from Ref. [26] for the *higher-latitude tail* and the preliminary results by the *Fermi*-LAT team [17] on the Galactic center include an estimate of the impact of foreground systematics. In these cases, the adopted ROIs are shown as bands (for Ref. [26], overlapping regions correspond to the north and south parts of the sky). *Gray areas* indicate the intensity level of the *Fermi* bubbles, extrapolated from $|b| > 10°$, and the region where HI and H2 gas emission from the inner Galaxy becomes important.

putative excess emission is – compared to other foregrounds/backgrounds – strongest, so the uncertainties due to foreground/background subtraction systematics are expected to be the smallest.

The intensities were derived by a careful rescaling of results in the literature that fully takes into account the assumed excess profiles. In most works, intensities are quoted as averaged over a given Region Of Interest (ROI). Instead of showing these averaged values, which depend on the details of the adopted ROI, we use the excess profiles to calculate the differential intensity at a fixed angular distance from the GC. These excess profiles usually follow the predictions similar to those of a DM annihilation profile from a generalized Navarro-Frenk-White (NFW) density distribution, which is given by

$$\rho(r) = \rho_s \frac{r_s^3}{r^\gamma (r + r_s)^{3-\gamma}} \,. \qquad (1)$$

Here, r_s denotes the scale radius, γ the slope of the inner part of the profile, and ρ_s the scale density. As reference values we will – if not stated otherwise – adopt $r_s = 20$ kpc and $\gamma = 1.26$, and ρ_s is fixed by the requirement that the local DM density at $r_\odot = 8.5$ kpc is $\rho_\odot = 0.4$ GeV cm^{-3} [95, 96].

We note that the intensities that we quote from Ref. [26] refer already to a $\bar{b}b$ spectrum and take into account correlated foreground systematics as discussed below. In Ref. [26] a broken power-law was found to give a fit as good as the DM $\bar{b}b$ spectrum. Assuming a broken power-law, the intensities in Fig. 1 would be somewhat larger.

We find that all previous and current results (with the exception of Ref. [7], which we do not show in Fig. 1) agree within a factor of about two with a signal morphology that is compatible with a contracted NFW profile with slope $\gamma = 1.26$, as it was noted previously [15, 26]. As mentioned in our Introduction, the indications for a higher-latitude tail of the GeV excess profile is a rather non-trivial test for the DM interpretation and provides a serious benchmark for any astrophysical explanation of the excess emission. However, we have to caution that most of the previous analyses make use of the *same* model for Galactic diffuse emission (`P6V11`). An agreement between the various results is hence not too surprising. Instead in the work of Ref. [26], the π^0, bremsstrahlung and ICS emission maps, where calculated as independent components, with their exact morphologies and spectra as predicted from a wide variety of foreground/background models. As it was shown in Ref. [26], the exact assumptions on the CR propagation and the Galactic properties along the line-of-sight can impact both the spectrum and the morphology (which also vary with energy) of the individual gamma-ray emission maps. To probe the associated uncertainties on those diffuse emissions, the authors of Ref. [26] built differ-

ent models allowing for extreme assumptions on the CR sources distribution and injection spectra, on the Galactic gasses distributions, on the interstellar radiation field properties, on the Galactic magnetic field magnitude and profile and on the Galactic diffusion, convection and reacceleration.

Having performed these tests, it is reassuring that Ref. [26] and later on Ref. [17], which employs an independently derived array of foreground/background models, find – in their respective ROIs and around 2 GeV – results that agree both in morphology and intensity of the *Fermi* GeV excess emission, between themselves and with previous works.[2]

In Fig. 1, we also indicate the latitude regions where the flux from the *Fermi* bubbles becomes important (at $|b| \gtrsim 14^\circ$, assuming a uniform intensity extrapolated from higher latitudes) and where strong emission from HI+H2 gas in the inner Galaxy might significantly affect the results (the inner 0.2 kpc). It appears that the latitude range $2^\circ \leq |b| \leq 15^\circ$ is best suited to extract spectral information about the GeV excess.

Despite the agreement, from Fig. 1 it is also evident that the exact values of the intensities disagree with each other at the $> 3\sigma$ level. Since most of the error bars are statistical only, this confirms that systematic uncertainties in the subtraction of diffuse and point source emission play a crucial role for the excess intensity. *These effects will be even more important for the spectral shape of the excess.* We will concentrate on the implication of Galactic diffuse model systematics for DM models in the next two sections III and IV.

III. THE TAILS IN THE *FERMI* GEV EXCESS SPECTRUM

As already mentioned, the spectrum of the *Fermi* GeV excess can be significantly affected by the uncertainties in the modeling of the Galactic diffuse emission (which, along the line-of-sight, is typically a factor of a few larger than the excess intensity). In general, the relevant diffuse foregrounds/backgrounds result from three processes: (1) the "π^0 emission", consisting of gamma rays from boosted neutral mesons (mainly π^0s) that are produced when CR nucleons have inelastic collisions with the interstellar gas, (2) the bremsstrahlung radiation of CR electrons when they scatter off those same interstellar gasses, and (3) the ICS, in which CR electrons up-scatter

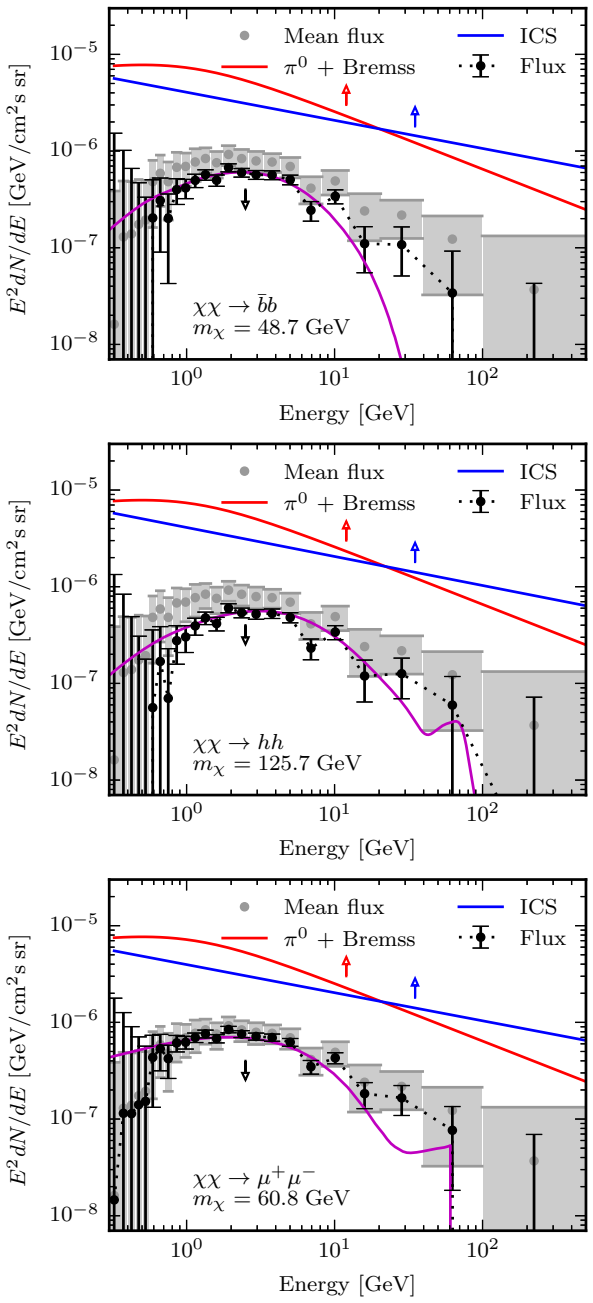

FIG. 2. The foreground/background systematics as derived in Ref. [26] allow a large number of DM annihilation channels to fit the data. This is here illustrated for three best-fit channels from Tabs. I and II (taking model F). Correlated systematics are shown by the *gray bands*, uncorrelated statistical errors by the error bars (including also remaining method uncertainties [26]), and we show the estimated ICS and π^0+Bremss foreground/background fluxes for comparison. As illustrated by the *black dots*, a small *increase* of these estimated Galactic diffuse emissions within their systematic uncertainties (barely visible on the log-scale) leads to a *decrease* of the inferred *Fermi* GeV excess flux and vice-versa. The magnitude of this effect is dependent on the fitted spectrum (and hence different in the three panels), but automatically taken into account when the full covariance matrix is used. Fluxes are averaged over $|l| < 20^\circ$ and $2^\circ < |b| < 20^\circ$.

[2] Although the intensity of the *Fermi* GeV excess that was found in Ref. [17] agrees at 2 GeV with previous findings, one has to be careful with using the preliminary energy spectra presented in that work for spectral studies. In particular for two of the presented background models, the spectral slopes of the background components were explicitly not tuned to match the observations. This may bias the residual gamma-ray excess towards higher energies, which could lead to biased results when fitting the excess spectrum.

cosmic microwave background and interstellar radiation field photons to gamma-ray energies. The first two contributions trace with good accuracy the Galactic gas distribution and, as a consequence, they are filamentary in their morphology. The ICS component, instead, is much more diffuse and could potentially contaminate or even mimic diffuse signals from DM annihilation.

In most of the previous studies on the GeV excess [11, 12, 14, 15, 24] the contribution from the Galactic diffuse emission has been modeled by using the `P6V11` model provided by the *Fermi*-LAT Collaboration.[3] This model was originally developed to subtract the diffuse gamma-ray background for point-like source emission studies, and its authors explicitly warn against using it for the study of extended diffuse contributions. Ref. [26] showed that the `P6V11` model has an unusually hard ICS component at energies above 10 GeV (this is not apparent on first sight, since ICS, π^0 and bremsstrahlung components are not separate in this model). In template regression analyses, this is likely to lead to over-subtracting the emission above 10 GeV, leading to artificial cutoffs in the GeV excess template at these energies.

In Fig. 2, we show the energy spectrum of the *Fermi* GeV excess as derived in Ref. [26], including systematic and statistical errors, compared to various DM annihilation spectra that we will discuss further below. In contrast to previous analyses, we find a clear *power-law like tail* at energies above 10 GeV. However, foreground/background model uncertainties introduce large uncertainties that are *correlated between the energy bins*. Their effect on the fitted spectrum is rather simple to understand and illustrated in the various panels of Fig. 2. The main foreground/background components are ICS, π^0 and bremsstrahlung. At first order, the modeling of these components can be off in their normalization or their slope, leading to residuals in the fit to the data that are partially absorbed by the *Fermi* GeV excess template. Ref. [26] estimated the size of this effect from a study of residuals along the Galactic disk, and showed that it can lead to a broadening or narrowing of the *Fermi* GeV excess spectrum, as shown in Fig. 2. An immediate implication is that, in light of these uncertainties, the *Fermi* GeV excess spectrum can be fit reasonably well with a broken power-law and different spectra from DM annihilation models.[4]

The impact of foreground/background model uncertainties on the *Fermi* GeV excess spectrum can be parametrized in terms of the covariance matrix of the flux uncertainties. The principal components of the covariance matrix reflect the above background variations, which we found to be at the few percent level [26]. Fits to the *Fermi* GeV excess spectrum are then performed using this simple χ^2 function,

$$\chi^2 = \sum_{ij} (\mu_i - f_i) \Sigma_{ij}^{-1} (\mu_j - f_j) \,, \qquad (2)$$

where μ_i and f_i are the modeled and the measured flux in the $i^{\rm th}$ energy bin, and Σ is the covariance matrix.

Best-fit parameters and their uncertainties are then as usual derived by minimizing the χ^2 function w.r.t. all model parameters, and determining the $\Delta\chi^2$ contours while profiling over the other parameters to infer confidence regions.

IV. IMPLICATIONS FOR MODELS OF ANNIHILATING DARK MATTER

In typical DM scenarios, gamma rays are produced via a variety of mechanisms. As DM particles annihilate, they produce Standard Model (SM) particles such as quarks, gluons, gauge bosons and leptons. These SM particles then hadronize and/or decay producing lighter mesons that give rise to a continuous spectrum of gamma rays. Moreover, $\mathcal{O}(\alpha_{\rm EM})$ corrections to the two-body final state annihilation process generate gamma rays when an additional photon or an SU(2) gauge boson is emitted. Finally, at the loop level, gamma-ray lines are expected from generic WIMP models. In particular, gamma rays from loop processes or emitted via electromagnetic virtual internal bremsstrahlung (VIB) and final state radiation (FSR) give hard spectra with evident cutoffs at the mass threshold, although suppressed in intensity. Both, higher order correction photons and the continuous spectrum, are emitted where the annihilation takes place and thus probe directly the annihilation rate profile. Typically, all these components are referred to as *prompt emission*.

The gamma-ray differential intensity (with units $\mathrm{GeV}^{-1}\,\mathrm{cm}^{-2}\,\mathrm{s}^{-1}\,\mathrm{sr}^{-1}$) from the annihilation of self-conjugate DM χ is

$$\frac{dN}{dE} = \sum_f \frac{\langle\sigma v\rangle_f}{8\pi\, m_\chi^2} \frac{dN_\gamma^f}{dE} \int_{\rm l.o.s} ds\, \rho^2(r(s,\psi)) \,, \qquad (3)$$

where the sum extends over all possible annihilation channels with final state f, $\langle\sigma v\rangle_f$ is the annihilation cross-section and dN_γ^f/dE is the DM prompt gamma-ray spectrum per annihilation to final state f. In this work, the DM prompt emission spectra for all channels except u, d and s quarks (generically $\bar{q}q$) and hh are computed from the tabulated spectra provided by `DarkSUSY` [97], which, in turn, derives the dN_γ^f/dE from `PYTHIA 6.4` [98]. We use the $\bar{q}q$ and hh spectra from `PPC4DMID` [99] (as are not included in the `DarkSUSY` tables), which makes use of `PYTHIA 8.135` [100]. For annihilation to bosons (W, Z and h) and t quarks, we checked

[3] `http://fermi.gsfc.nasa.gov/ssc/data/P6V11/access/lat/ring_for_FSSC_final4.pdf`

[4] Ref. [26] also estimated the uncertainties of the *low-energy (sub-GeV) tail* of the spectrum. These uncertainties are mostly coming from the masking of point sources. The corresponding increase of the errors is shown in Fig. 2. At the lowest energies, only upper limits on the flux can be derived.

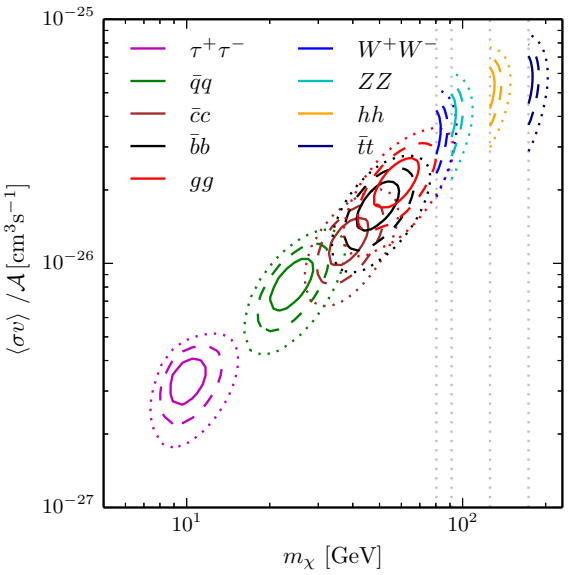

FIG. 3. Preferred DM mass and annihilation cross-section (1, 2 and 3 σ contours) for all single channel final states where ICS emission can be safely ignored. *Vertical gray lines* refer to the W, Z, h and t mass thresholds. The p-values for annihilation to pure W^+W^-, ZZ and $\bar{t}t$ final states are below 0.05, indicating that the fit is poor for these channels; see Tab. I. Uncertainties in the DM halo of the Milky Way are parametrized and bracketed by $\mathcal{A} = [0.17, 5.3]$, see Sec. V. The results shown here refer to $\mathcal{A} = 1$.

Channel	$\langle\sigma v\rangle$ (10^{-26} cm^3 s^{-1})	m_χ (GeV)	$\chi^2_{\rm min}$	p-value
$\bar{q}q$	$0.83^{+0.15}_{-0.13}$	$23.8^{+3.2}_{-2.6}$	26.7	0.22
$\bar{c}c$	$1.24^{+0.15}_{-0.15}$	$38.2^{+4.7}_{-3.9}$	23.6	0.37
$\bar{b}b$	$1.75^{+0.28}_{-0.26}$	$48.7^{+6.4}_{-5.2}$	23.9	0.35
$\bar{t}t$	$5.8^{+0.8}_{-0.8}$	$173.3^{+2.8}_{-0}$	43.9	0.003
gg	$2.16^{+0.35}_{-0.32}$	$57.5^{+7.5}_{-6.3}$	24.5	0.32
W^+W^-	$3.52^{+0.48}_{-0.48}$	$80.4^{+1.3}_{-0}$	36.7	0.026
ZZ	$4.12^{+0.55}_{-0.55}$	$91.2^{+1.53}_{-0}$	35.3	0.036
hh	$5.33^{+0.68}_{-0.68}$	$125.7^{+3.1}_{-0}$	29.5	0.13
$\tau^+\tau^-$	$0.337^{+0.047}_{-0.048}$	$9.96^{+1.05}_{-0.91}$	33.5	0.055
$[\mu^+\mu^-$	$1.57^{+0.23}_{-0.23}$	$5.23^{+0.22}_{-0.27}$	43.9	0.0036$]_{\cancel{\rm ICS}}$

TABLE I. Results of spectral fits to the *Fermi* GeV excess emission as shown in Fig. 2, together with $\pm1\sigma$ errors (which include statistical as well as model uncertainties, see text). We also show the corresponding p-value. Annihilation into $\bar{q}q$, $\bar{c}c$, $\bar{b}b$, gg and hh all give fits that are compatible with the observed spectrum. There is also a narrow mass where annihilation into $\tau^+\tau^-$ is *not* excluded with 95% CL significance. Annihilation to pure W^+W^-, ZZ and $\bar{t}t$ is excluded at 95% CL, as is the $\mu^+\mu^-$ spectrum *without* ICS emission ($\cancel{\rm ICS}$). Bosons masses are from the PDG live [101].

that the interpolation at mass threshold agrees with our own results from `PYTHIA 8.186`.

In addition to gamma rays, CR electrons and positrons are produced as final (stable) products of DM annihilations. These CR electrons/positrons, like all other electrons/positrons propagate in the Galaxy and produce ICS and bremsstrahlung emission.[5] Generally, the ICS emission is expected to be more important for DM models with significant branching ratios to (light) leptons. Therefore we separate our discussion to first address the cases when ICS emission can be safely ignored, before discussing in detail ICS emission for annihilation to leptons.

A. Single annihilation channels without ICS

We first discuss annihilation to pure two-body annihilation states for the cases when ICS emission can be safely ignored. This turns out to be all cases except annihilation to electrons and muons. In Fig. 3 we show the best-fit annihilation cross-section and DM mass for all other two-body annihilation states involving SM fermions and bosons. The results are also summarized in Tab. I, where we furthermore give the p-value of the fit as a proxy for the goodness-of-fit. As with previous analyses, we find that annihilation to gluons and quark final states $\bar{q}q$, $\bar{c}c$ and $\bar{b}b$, provides a good fit. In the case of the canonical $\bar{b}b$ final states, we find slightly higher masses are preferred compared to previous analyses, see *e.g.* Refs. [12, 14, 15]. This is because of the additional uncertainty in the high-energy tail of the energy spectrum that is allowed for in this analysis. The highest mass to $\bar{b}b$ final states that still gives a good fit (with a p-value > 0.05) is 73.9 GeV.

As the tail of the spectrum extends to higher energy, we also consider annihilation to on-shell $\bar{t}t$ and SM bosons. For $\bar{t}t$, we find that the fit is poor because the DM spectrum peaks at too high an energy (~ 4.5 GeV rather than the observed peak at 1–3 GeV). As the p-value is very low for this channel, we do not consider it further. Pure annihilation to pairs of W and Z gauge bosons are also excluded at a little over 95% CL significance. However, perhaps surprisingly, annihilation to pairs of on-shell Higgs bosons (colloquially referred to as "Higgs in Space" [102]) produce a rather good fit, so long as h is produced close to rest. This is analogous to the scenario studied in Ref. [103] in a different context. One interesting feature of this channel is the gamma-ray line at $m_\chi/2 \simeq 63$ GeV from h decay to two photons. This is clearly visible in the central panel of Fig. 2. The branching ratio for $h \to \gamma\gamma$

[5] CR p and $\bar{p}$ from DM annihilations can also give their own π^0 emission of DM origin, but are suppressed from the $\bar{p}/p$ measurements already by at least five orders of magnitude compared to the conventional Galactic diffuse π^0 emission.

Diffuse Model	$\langle\sigma v\rangle$ (10^{-26} cm^3 s^{-1})	m_χ (GeV)	$\chi^2_{\rm min}$	p-value
A	$12.4^{+1.6}_{-1.6}$	$71.2^{+5.6}_{-4.8}$	34.4	0.04
C	$11.8^{+3.3}_{-3.3}$	$75.2^{+7.9}_{-8.1}$	77.5	$\ll 10^{-3}$
D	$3.56^{+0.44}_{-0.44}$	$57.4^{+4.6}_{-4.1}$	23.9	0.35
F	$1.70^{+0.22}_{-0.22}$	$60.8^{+5.8}_{-3.9}$	28.2	0.17

TABLE II. Results of spectral fits to the *Fermi* GeV excess emission for 100% annihilation into $\mu^+\mu^-$, with ICS emission modeled according to Galactic diffuse models A, C, D and F (see Ref. [26]). The $\pm1\sigma$ errors include statistical as well as model uncertainties, see text. We also show the minimum χ^2, and the corresponding p-value.

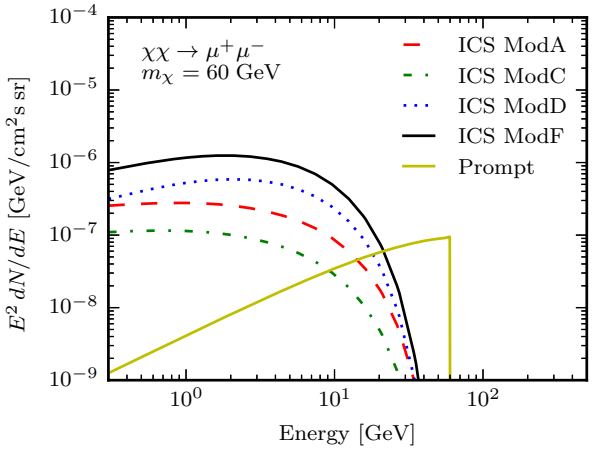

FIG. 4. The ICS emission spectrum from propagation models A, C, D and F (see Ref. [26]) for a DM particle of 60 GeV annihilating to $\mu^+\mu^-$ with thermal cross-section. Fluxes are averaged over a $40^\circ \times 40^\circ$ ROI centered on the GC, with $|b| < 2^\circ$ masked. For comparison, we also show the prompt component of that channel, which is dominated by final state radiation.

is 2.3×10^{-3}. Following Tab. I, this implies a partial annihilation cross-section into four photons with $m_\chi/2$ energy of $\langle\sigma v\rangle_{\gamma\gamma\gamma\gamma} \simeq 1.2 \times 10^{-28}$ cm^3 s^{-1}. Relevant limits from gamma-ray line searches can be found for example in Ref. [104] (see also Ref. [21]). For a contracted NFW profile (rescaled to $\gamma = 1.26$), the limit for 125.7/2 GeV mass DM particles annihilating into two photons with energy 125.7/2 GeV is $\langle\sigma v\rangle_{\gamma\gamma} \lesssim 4.2 \times 10^{-29}$ cm^3 s^{-1} (at 95% CL). The relevant limit in our case is that $\langle\sigma v\rangle_{\chi\chi\to hh\to\gamma\gamma\gamma\gamma} \lesssim 8.4\times10^{-29}$ cm^3 s^{-1}: there is a factor 2 because there are four γ in each annihilation instead of two, but this is compensated by a factor 1/4 from the reduction in the DM number density because, to produce photons with the same energy, the DM must be twice as heavy in $\chi\chi \to \gamma\gamma\gamma\gamma$ compared to $\chi\chi \to \gamma\gamma$. We find that $\langle\sigma v\rangle_{\gamma\gamma\gamma\gamma}$ is therefore just below current limits. It should be remembered that if the Higgs particles are not produced exactly at rest, the lines are somewhat broadened, which reduces the sensitivity of line searches [105].

We next turn to consider annihilation to leptons. Owing to the larger foreground uncertainties in this analysis, we find that there is a small mass window where $\tau^+\tau^-$ final state has a p–value larger than 0.05 (from about 9.4 GeV up to 10.5 GeV).

For completeness, we also list in Tab. I the result of our spectral fit to $\mu^+\mu^-$ final states *without accounting for ICS emission*.

Finally, we remind the reader that the quoted cross-sections assume the Milky Way halo parameters detailed in Sec. II. These halo parameters are not well known and as we will discuss below in Sec. V, dynamical and microlensing constraints on the halo parameters (from [106]) translate to about a factor five uncertainty in the cross-section in both directions.

B. Single annihilation channels with ICS

ICS emission is expected to be important for DM models with significant branching ratios to (light) leptons (see for instance Ref. [107] for a discussion in the context of the GeV excess at the GC). Yet, any DM model that has a large branching ratio to monochromatic e^+e^- is severely constrained by the positron fraction data from the AMS experiment [82]. Moreover, for any DM mass the annihilation channel to monochromatic e^+e^- would lead to an ICS gamma-ray spectrum with a hard cutoff at the mass threshold. This though is in tension with the fact that the *Fermi* GeV excess spectrum has a very broad peak at $\simeq 2$ GeV, making such a model an improbable one in the context of the *Fermi* GeV excess. Therefore, DM models annihilating into e^+e^- will not be studied in this work. We concentrate instead on the ICS signatures from DM annihilations to $\mu^+\mu^-$.

For the calculation of the ICS spectrum of DM origin we use `GALPROP v54.1.984`[6] [108, 109]. The ICS signal depends on the assumptions with regards to the photon targets of the interstellar radiation field and those on the energy losses and diffusion time scales of the electrons/positrons. We use in this work four different Galactic diffuse emission (Galactic CR propagation) models that account for the relevant uncertainties. These four models are models A, C, D and F of Ref. [26]. As can be seen in Fig. 4, these four models give significantly different predictions (by almost an order of magnitude) for the averaged (over our ROI) ICS DM signal. Finally, bremsstrahlung of DM origin is insignificant in all these cases and thus can be ignored.[7]

[6] `http://galprop.stanford.edu/`

[7] We find the ratio of ICS/bremsstrahlung flux to be between 10 and 100, for all the relevant DM annihilation modes and for gamma-ray energies < 10 GeV that affect the spectral fits.

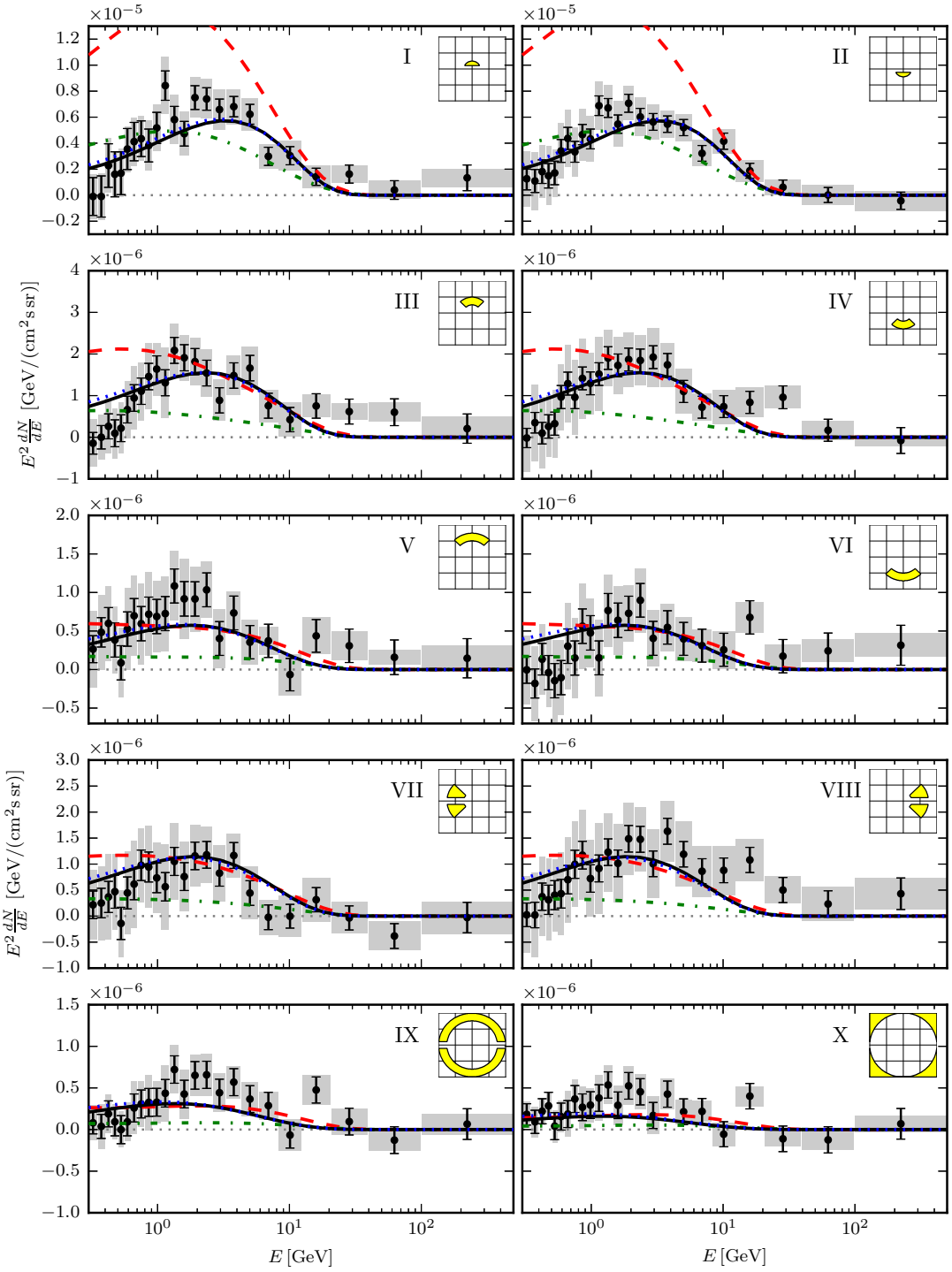

FIG. 5. For the same mass and cross-section as in Tab. II the DM signal versus the gamma-ray *Fermi* GeV excess data for the ten sub-regions of Ref. [26] and for the four diffuse emission models adopted (same color/line style as in Fig. 4). In the case of model A (*red dashed line*), while averaged over the entire ROI, the gamma-ray DM signal from the specific choice of mass and cross-section for this channel provides a good fit, once further scrutinized to the ten sub-regions, this DM model is excluded. On the other hand, model D (*blue dotted line*) and F (*black solid line*) still provide a signal compatible with the measured one in each of the 10 sub-regions. The insets show the geometry of the regions in a $40^\circ \times 40^\circ$ box centered on the GC; see also Tab. III.

As for annihilation into two-body final states, the ICS emission plays an important role for the $\mu^+\mu^-$ channel. Annihilation into $\mu^+\mu^-$ is excluded with high confidence level (p-value of 0.0036) when only the prompt emission is considered, as can be see in Tab. I. Instead, the inclusion of the ICS component significantly improves the fit. Tab. II quotes the best-fit parameter values and p-values for annihilation into $\mu^+\mu^-$ when the ICS emission is modeled according to the four different propagation models introduced above. The effect of ICS inclusion is two-fold: First, the best-fit mass range is shifted towards higher masses ($\sim$ 60–70 GeV), while the best-fit cross-section value can vary by about a factor of ten depending on the model. Second, it is possible to find models for which the goodness-of-fit is improved and can become competitive with annihilation to $\bar{b}b$, $\bar{c}c$, light quarks and gluons (compare models D and F for the $\mu^+\mu^-$ channel from Tab. II to the relevant channels of Tab. I). The reason why such a possibility opens is that, as shown in the lower panel of Fig. 2 and Fig. 4, the combined ICS and prompt gamma-ray spectrum can be significantly altered with the ICS smooth bump dominating in the fit over the FSR hard spectral feature. This is the case for certain Galactic diffuse emission model assumptions; the model must allow for the injected electrons/positrons from DM annihilation to lose most of their energy via ICS emission. If CR electrons and positrons instead have large diffusion time scales (slow diffusion) and/or lose most of their energy via the competing synchrotron losses, the ICS at higher latitudes will be strongly suppressed.

For channels that have significant ICS emission, it is not enough to fit the spectral energy distribution, but also the morphology of the signal has to be checked. Indeed, as mentioned above, the ICS emission is strictly correlated with the distribution of the ambient photons. Thus, the morphology of the emission associated with ICS emission could in principle be different with the morphology of the GeV excess.[8] For this reason, in Fig. 5 we show the results of the fits in the ten ROIs used in Ref. [26] to characterize the morphology of the GeV excess. The definition of the ten ROIs allowed us to study the symmetry properties of the excess and its extension in latitude. For the sake of completeness, we quote in Tab. III the definition of the ten ROIs as in Ref. [26]. In each sub-region we display the GeV excess data together with the ICS emission from $\mu^+\mu^-$ annihilation for the four Galactic diffuse emission models A, C, D and F, and for the DM masses and cross-sections quoted in Tab. II. Models D and F are able to reproduce the correct morphology of the excess, while models A and C fail in this respect. The plot is illustrative of the fact that it is possible to find propagation models for which the morphological properties of the GeV excess are recovered. Thus, it is not possible to exclude ICS emission from muons only on the basis of gamma-ray data.

ROI	Definition
I, II	$\sqrt{\ell^2+b^2} < 5^\circ$, $\pm b > 2^\circ$
III, IV	$5^\circ < \sqrt{\ell^2+b^2} < 10^\circ$, $\pm b > \lvert\ell\rvert$
V, VI	$10^\circ < \sqrt{\ell^2+b^2} < 15^\circ$, $\pm b > \lvert\ell\rvert$
VII, VIII	$5^\circ < \sqrt{\ell^2+b^2} < 15^\circ$, $\pm \ell > \lvert b\rvert$
IX	$15^\circ < \sqrt{\ell^2+b^2} < 20^\circ$
X	$20^\circ < \sqrt{\ell^2+b^2}$, $\lvert b\rvert < 20^\circ$, $\lvert\ell\rvert < 20^\circ$

TABLE III. Definition of the ten ROIs used in Ref. [26] for the morphological analysis of the excess. Table adapted from Ref. [26].

Other important constraints on DM annihilating to muons come from the CR positron fraction measured by AMS-02 [82]. For model F the combination of best-fit cross-section and mass in Tab. II is still allowed at 95% CL, once uncertainties on the local DM density and local CR electrons energy losses are taken into account. Instead, models A and C are already in strong tension. An appealing feature of this channel is that anti-proton constraints [84–88, 90] do not apply. Before drawing any final conclusion about the possibility of having annihilation into muons it is also important to test synchrotron radiation. This is beyond the scope of the present paper and will be addressed in a dedicated work.[9]

We briefly mention why ICS emission is not important for annihilation into light quarks or $\tau^+\tau^-$. For annihilations into light quarks and gluons, only $\sim 1/6$ of the available energy per annihilation goes to e^+e^- after all the hadronization and decay processes have occurred. Moreover the spectra of these e^+e^- tend to be soft at injection, resulting in an ICS signal that is subdominant compared to the gamma-ray prompt emission signal around the energies of the *Fermi* GeV excess. For direct annihilation to $\tau^+\tau^-$, while a significant portion of the annihilation power does go into e^+e^-, the prompt gamma-ray emission has a very prominent spectral bump, that cannot be "smoothed out" significantly by including the ICS contribution. In these cases, we have checked that including the ICS emission impacts the best-fit mass and cross-section in Tab. I and their respective 1, 2 or 3 σ ranges in Fig. 3 by no more than 5%.

Finally we notice that for a point-like source of high energy electrons located at the GC, either at a steady rate or for a sequence of burst-like events with a time-scale separation between the events of $\sim \mathcal{O}(100)$ kyr or less, the simultaneous explanation of the spectrum in the entire ROI of Ref. [26] ($|l| < 20^\circ$, $2^\circ < |b| < 20^\circ$) and

[8] The prompt-only component does not have such a drawback as a consequence of the fact that the prompt photons directly trace the DM distribution in the Galaxy.

[9] It may also be interesting to include the bremsstrahlung emission in some cases [110].

its ten sub-regions is going to be challenging. We expect for the ICS signature, even if it fits the entire ROI, it will overshoot the data in the inner sub-regions (mainly regions I and II) and undershoot the outer sub-regions data, much like in Galactic diffuse emission model A of Fig. 5.

C. Mixed annihilation channels

The discussion so far has focused on annihilation into a single channel of final states. In a realistic model, DM will likely annihilate into a variety of channels with different branching ratios, defined as $\mathrm{BR}(\bar{f}f) = \langle\sigma v\rangle_f / \sum_f \langle\sigma v\rangle_f$ where the sum extends over all available channels. For instance, all but two of the models in Refs. [34–77] annihilate into multiple final states (the exception being flavored DM models [49, 50], where annihilation into only $\bar{b}b$ is possible).

Previous multi-channel fits to the GeV excess have generally focused on the cases where $\langle\sigma v\rangle_f \propto \{m_f^2, e_f^2, \mathbb{1}\}$, where m_f is the final state mass, e_f the final state electric charge and $\mathbb{1}$ denotes universal couplings. These scenarios can be motivated by considering models where the particle mediating the annihilation mixes with the SM Higgs (in variations of two-Higgs doublet (2HDM) or Higgs portal models [111]) or from Minimal Flavor Violation [112] (in the case $\langle\sigma v\rangle_f \propto m_f^2$), where a vector mediator kinetically mixes with electromagnetism (when $\langle\sigma v\rangle_f \propto e_f^2$) or where the couplings are assumed universal as a simplifying assumption (when $\langle\sigma v\rangle_f \propto \mathbb{1}$). Here however, we remain more agnostic to the allowed final states. We do this for two reasons: Firstly, models often predict deviations from the exact relations $\langle\sigma v\rangle_f \propto \{m_f^2, e_f^2, \mathbb{1}\}$. Secondly, not all models have been explored so we do not want to over restrict ourselves.

We therefore show in Figs. 6 and 7 triangle plots with fits to three final state channels. The plots are such that the branching ratios (BR) sum to one (as required) and we have marginalized over the DM mass and the total annihilation cross-section. Owing to the large uncertainty on the total cross-section from the Milky Way halo parameters (about a factor five as we anticipated in Fig. 3 and discussed in Sec. V), we choose to show the DM mass that minimizes the χ^2 at each point by means of the background coloring.

Fig. 6 focuses on the case of annihilation to quark and lepton channels. The top-left triangle is for quark-only final states (we don't consider gg as it is loop suppressed so its branching ratio is naturally smaller). As each channel individually gives a good fit, it is no surprise that any combination of $\bar{q}q$, $\bar{c}c$ and $\bar{b}b$ also gives a good fit with DM in the mass range between 25 and 60 GeV. The top-right triangle is for heavy quark and τ final states, as would be expected for 2HDM and Higgs-portal models with $m_\chi < m_t$. The best-fit point lies close to the ratios predicted in these models $\bar{b}b : \bar{c}c : \tau^+\tau^- = 0.87 : 0.08 : 0.05$. We also find that $\mathrm{BR}(\tau^+\tau^-)$ can be substantial (up to around 75%) while still providing a good spectral fit (p-value > 0.05). The bottom two triangles consider annihilation channels involving muons, where we include ICS emission assuming propagation model F. Considering first the case of annihilation into $\mu^+\mu^-$ and $\tau^+\tau^-$ only (along the axis $\mathrm{BR}(\bar{q}q) = 0$), we see that a good fit can always be obtained when $\mathrm{BR}(\mu^+\mu^-) \gtrsim 0.6$ and $m_\chi \sim 50$ GeV. Constructing models giving only $\mu^+\mu^-$ and $\tau^+\tau^-$ final states may be challenging but see Ref. [41] for a prototype. When allowing for additional annihilation into $\bar{q}q$ or $\bar{b}b$, we find that all values of $\mathrm{BR}(\mu^+\mu^-)$ result in a good fit.

In Fig. 7 we consider final states which contain at least one heavy boson. The single channel annihilation to W^+W^- or ZZ is just excluded at 95% CL, therefore in the upper triangle we investigate whether a combination of $\bar{b}b$ in addition to W^+W^- and ZZ improves the fit. Unfortunately we find that this is not the case: the best-fit point remains pure annihilation to ZZ. We find the same conclusion for annihilation to other light quark anti-quark pairs (not shown). This is expected because of the constraints imposed on the DM mass, $m_\chi > m_Z$ (due to the requirement of producing the heavy bosons on shell).

In Sec. IV A, we found that single channel annihilation to hh gives a fit that it compatible with the observed energy spectrum. In the middle and lower triangles we investigate if the inclusion of additional quark and lepton final states, and additional W^+W^- and ZZ final states improves the pure hh fit. A small fraction with $\bar{b}b$ provides a marginally better fit but generally – when adding both quark and leptons or heavy gauge bosons – we find that a good fit is obtained only when $\mathrm{BR}(hh) \gtrsim 0.8$ and when the DM mass is close to m_h (recall that also in this case the production of on-shell Higgs imposes $m_\chi > m_h$). This implies that simple models such as singlet scalar DM [113–116], which predicts sizable branching ratios to W^+W^-, ZZ and hh, are excluded since there $\mathrm{BR}(W^+W^-)$ is largest. Building realistic models that annihilate dominantly to hh may prove challenging, but opens to new, unexplored, possibilities.

D. Annihilation to hidden sector mediators

Up to this point we have only considered scenarios where the DM particles annihilate directly to SM particles. However it is also plausible that the DM first annihilates to intermediate hidden sector mediators ϕ that subsequently decay to SM particles. The mediator ϕ can mix with the SM Higgs or with hypercharge/electromagnetism, allowing for a variety of possible SM states from their decays.

These "cascade" annihilations produce boosted SM final states, which, depending on the ϕ mass, allow for heavier DM particles than in the more conventional scenarios discussed previously. The case in which a gen-

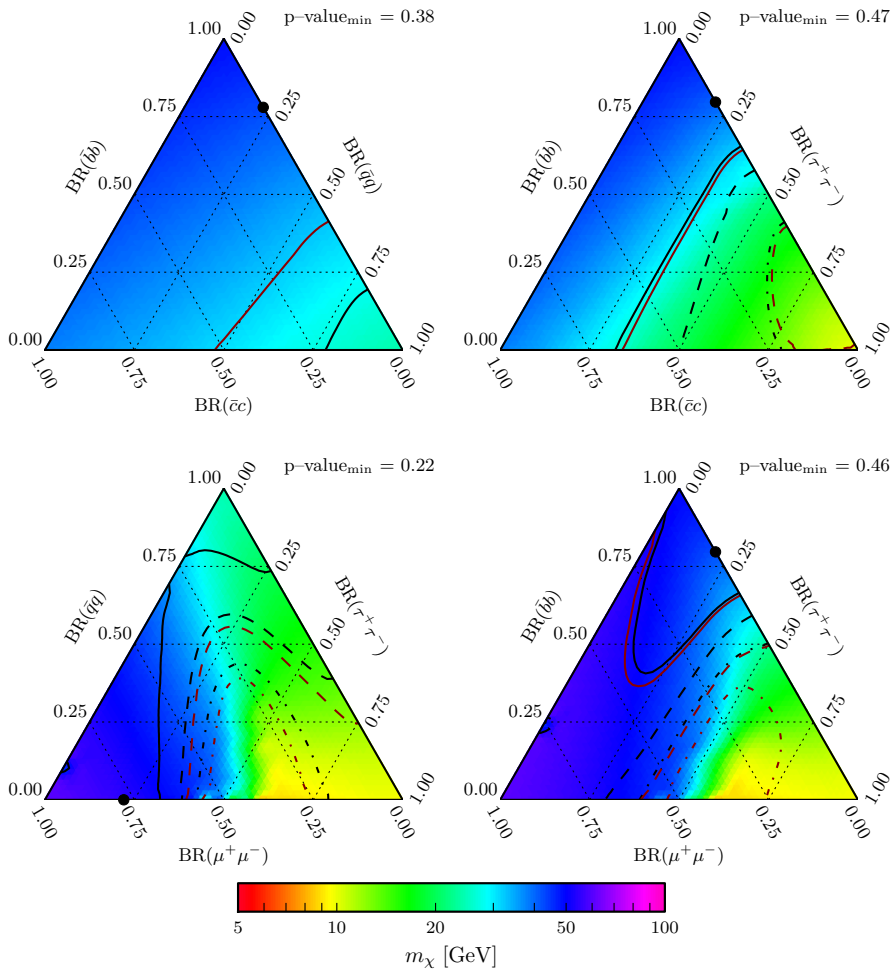

FIG. 6. Constraints on the branching ratio (BR) to mixed final states that include quarks and leptons. We marginalize over the DM mass and the total annihilation cross-section. The angles of each triangle represent annihilations to a pure channel, with the mass and cross-section being the best fit values given in Tabs. I and II (model F). The *black dot* in each plot corresponds to the best-fit point (we give the p-value here), the *solid*, *dashed* and *dot-dashed black lines* show the 1, 2, and 3 σ contours about the best-fit point, and the *solid*, *dashed* and *dot-dashed red lines* indicate p-value contours of 0.32, 0.05 and 0.01 respectively. Any combination of light quarks always results in a good fit. The BR to $\tau^+\tau^-$ can be substantial, with values over $\sim 50\%$ allowed at 2σ. Owing to the inclusion of ICS emission, any value of BR($\mu^+\mu^-$) results in a good fit (*cf.* bottom panels) when some fraction of $\bar{q}q$, $\bar{b}b$ or $\tau^+\tau^-$ is also included. In each panel the background coloring refers to the best-mass range as indicated by the color bar. Masses in the range 35–60 GeV lie inside the best-fit regions for all the shown combinations.

eral mediator ϕ decays primarily to b quarks has already been discussed extensively in the literature [53–55, 57, 59, 60, 70]. In fact the single channel annihilation to hh can be considered in this class since, after the h is produced, it decays dominantly to $\bar{b}b$ with each b having energy $m_h/2$. This is why a DM interpretation for this channel results in a good-fit even though the DM mass is over twice as heavy compared with the values for other channels.

Here we consider eXciting Dark Matter models (XDM)[117, 118]. For an earlier discussion of XDM models in the context of the *Fermi* GeV excess see [119]. If the gauge bosons ϕ are lighter than 2 GeV, the kinematically allowed final states are e^+e^-, $\mu^+\mu^-$ and $\pi^+\pi^-$ or π^0s, while no anti-protons are produced, thus evading the current constraints [120]. Such channels will produce, after all the subsequent cascades, boosted electrons and positrons and a subdominant contribution to FSR [121].

The π^0 channel can be evaded if the ϕ mixes with electromagnetism, thus coupling to charge [118]. We will therefore concentrate here on the annihilation channel $\chi\chi \to \phi\phi$, with subsequent ϕ decays as $\phi \to e^+e^-$, $\phi \to \mu^+\mu^-$ or $\phi \to \pi^+\pi^-$.[10]

[10] For a case where the π^0 modes dominate, see [122].

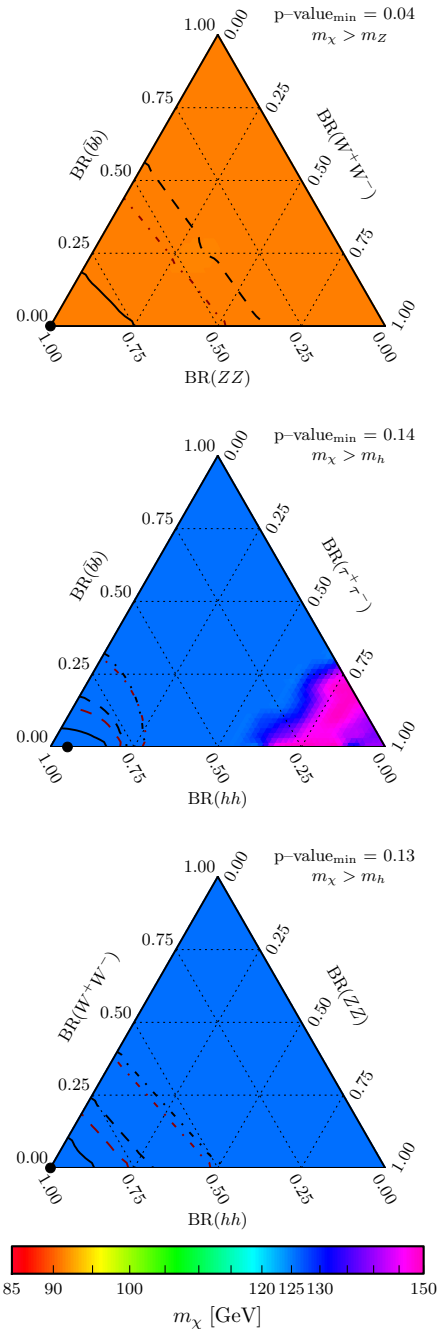

FIG. 7. Same as Fig. 6, but for a selection of mixed final states that include SU(2) gauge bosons and the Higgs channel on shell. *Upper panel:* We show the combination of heavy gauge bosons, W and Z, together with the possibility to annihilate into b quark final states. Given the imposed constraint $m_\chi > m_Z$, the best-fit region is forced to be close to the pure annihilation to ZZ. *Central panel:* We show a combination of b quarks, τ-leptons and hh. As above the constraint from the Higgs channel on the DM mass, $m_\chi > m_h$, causes the best-fit region to be close to the pure annihilation to hh. We notice that, when a substantial fraction of $\tau^+\tau^-$ is allowed, together with the mass constraint, the fit is very bad. *Lower panel:* We show the combination of W^+W^-, ZZ and hh annihilation states.

Channel	$\langle\sigma v\rangle$ (10^{-26} cm^3 s^{-1})	m_χ (GeV)	$\chi^2_{\rm min}$	p-value
$\phi \to e^+e^-$	$0.384^{+0.052}_{-0.051}$	$45.7^{+3.4}_{-3.3}$	31.35	0.09
$\phi \to \mu^+\mu^-$	$2.90^{+0.43}_{-0.42}$	$91.7^{+8.9}_{-7.5}$	33.6	0.05
$\phi \to \pi^+\pi^-$	$5.11^{+0.72}_{-0.71}$	$124.5^{+11.3}_{-9.8}$	33.3	0.06

TABLE IV. As in Tab. I, results of spectral fits to the *Fermi* GeV excess emission, for DM models annihilating into light bosons ϕ. The corresponding p-value is ≥ 0.05 in all cases. A slightly better fit is provided by $\phi \to e^+e^-$. For the ICS emission we considered the diffuse emission model F.

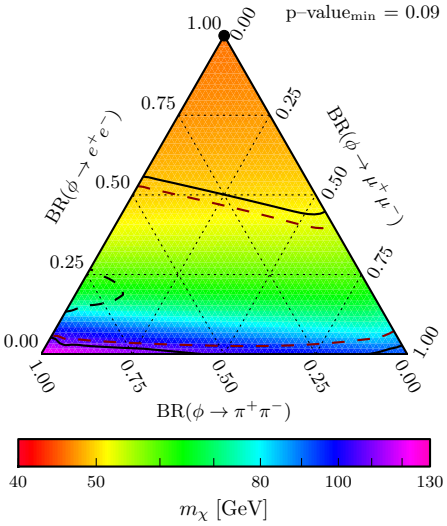

FIG. 8. Same as Fig. 6, but for annihilation into light bosons ϕ, which subsequently decay to $\phi \to e^+e^-$, $\phi \to \mu^+\mu^-$ and $\phi \to \pi^+\pi^-$. While the best fit case is for the pure case to $\phi \to e^+e^-$, at the 2σ level a wide variety of possible BRs and a range of masses between 45 GeV and 125 GeV is allowed.

As the final states contain light leptons, it is again crucial to include ICS emission. We do this as before using the Galactic diffuse emission model F. We show the results from our spectral fits in Tab. IV for single channel decay to each of the three possible ϕ decay modes: e^+e^-, $\mu^+\mu^-$ or $\pi^+\pi^-$. We find that the best-fit case, $\phi \to e^+e^-$, suggests a mass and a cross-section that is still allowed from AMS positron fraction limits, within their uncertainties, similarly to the case of direct DM annihilation to $\mu^+\mu^-$ discussed in Sec. IV B. Fig. 8 shows the resulting triangle plot for floating BRs between the three ϕ decay modes, after marginalizing over the DM mass and the annihilation cross-section to produce $\phi\phi$. Again the AMS positron fraction limits constrain (but not severely) these possibilities. For reference in these calculations we have chosen ϕ to be a vector with a mass of $\simeq 0.6$ GeV. Our spectral fit results do not depend on the exact value of the ϕ mass, as long as it remains within 0.3–1 GeV, and

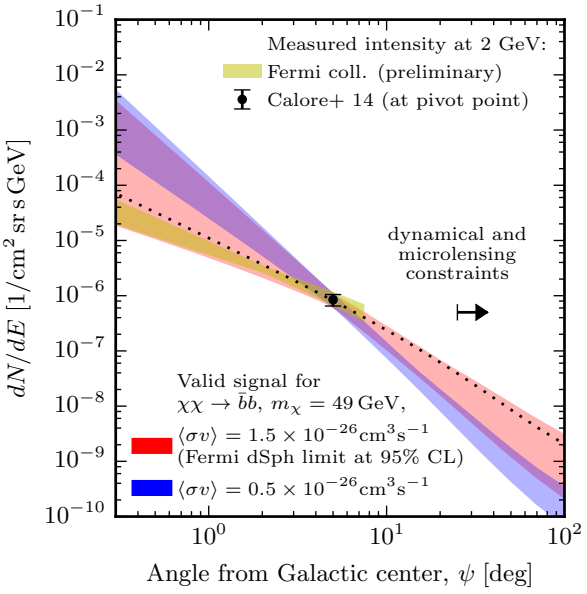

FIG. 9. Radial intensity profile of the *Fermi* GeV excess, at 2 GeV, *cf.* Fig. 1. The *black data point* refers to measurements from Refs. [26], the *yellow band* to preliminary results from the *Fermi*-LAT team [17]. The *dotted line* shows the expectations for a contracted NFW profile from Fig. 1. The *red* and *blue bands* show – for a given DM annihilation scenario – possible signal morphologies that are compatible with both the measurements at $\psi = 5^\circ$ as well as dynamical and microlensing observations from Ref. [106] (we concentrate on arbitrary generalized NFW profiles). For annihilation cross-sections close to the current dwarf limits, the intensities determined by different groups (as indicated by the dotted line), lie still in the allowed range.

on whether ϕ is a vector or a scalar, given the similarity of the injected electron/positron spectra into the interstellar medium from these options. Yet, on the model building side these can be important assumptions [118, 123].

V. CURRENT AND FUTURE CONSTRAINTS FROM DWARF SPHEROIDALS

The arguably most promising channel for a confirmation of the DM interpretation of the *Fermi* GeV excess are searches for corresponding signals in dwarf spheroidal galaxies of the Milky Way. These observations probe already – for typical assumptions on the Milky Way DM halo – DM scenarios that could explain the *Fermi* GeV excess [91–94]. The currently strongest (though still preliminary) limit on the annihilation cross-section was presented in Ref. [124]. For annihilation into $\bar{b}b$ final states and a DM mass of 49 GeV, they read $\langle\sigma v\rangle < 1.5 \times 10^{-26}$ cm^3 s^{-1} at 95% CL, which is at face-value in mild tension with the values of the cross-section that we derived above (see Sec. IV). However, the link between the GC and the dwarf signals is subject to uncertainties in the DM distribution in the Milky Way and the DM distribution in dSphs (note that the latter have been marginalized over in the analysis of Ref. [124]). Concerning the Milky Way halo, a decrease of the scale radius r_s, an increased slope γ of the inner part of the profile, or an increased local density $\rho_\odot$ enhance the expected GC signal relative to the signal in dwarf spheroidals. Also more cored profiles for dSphs can reduce further their constraining power. It is important to investigate to what extent uncertainties in these parameters can mitigate potential tensions between GC and dSph observations [125].

In Fig. 9 we show the *expected* signal flux for DM annihilation into $\bar{b}b$ final states and with $m_\chi = 48.7$ GeV. As DM profile we adopt here the reference generalized NFW profile as above and the cross-section is set to $\langle\sigma v\rangle = 1.75\times10^{-26}$ cm^3 s^{-1}. This leads to a signal intensity that is consistent with the results found in Ref. [26] at $\psi = 5^\circ$. Note that $\psi = 5^\circ$ was found to be a good pivot point for the intensity measurement in Ref. [26], as the flux there is relatively independent of the adopted profile slope. We also show the preliminary GC results by the *Fermi*-LAT Collaboration, *cf.* Fig. 1.

To explore the validity of measured signal profile, we generate a large set of Milky Way DM halo models that are compatible with the microlensing and dynamical constraints from Ref. [106] at 95% CL. This set includes DM halo models that follow a generalized NFW profile with scale radii in the range $r_s = 10$ to 30 kpc, and arbitrary normalization ρ_s and inner slope γ (note that for illustrative purposes we allow also values of γ that would be incompatible with the *Fermi* GeV excess measurements at the GC). To this end, we adopt the following method: We derive the envelope of all density profiles that are compatible with the left panel of Fig. 5 of Ref. [106] (which shows results for $r_s = 20$ kpc only) in the radial range $r = 2.5$ to 10 kpc. A model with scale radius $r_s \neq 20$ kpc is considered to be compatible with the observations when its profile lies within the derived envelope.

From the set of all observationally allowed halo models we select those that lead to a signal intensity that is consistent with the measurements at $\psi = 5^\circ$, assuming a reference cross-section $\langle\sigma v\rangle = 1.5 \times 10^{-26}$ cm^3 s^{-1} (the current dSph limit at 95% CL) and the above annihilation channel and DM mass. The envelope of the corresponding allowed signal profiles is shown by the red band in Fig. 9. The band contains both the signal morphology as derived for the reference generalized NFW profile with $\gamma = 1.26$, as well as with the preliminary GC results by the *Fermi*-LAT Collaboration. *We hence find that current dSph limits on the annihilation cross-section are well consistent with a DM interpretation of the Fermi GeV excess when uncertainties in the DM distribution in the Milky Way are accounted for.*[11]

[11] Note that this statement does not depend on the annihilation

The situation changes drastically however if current limits would increase by only a factor of three. This is demonstrated by the blue band in Fig. 9, which shows the corresponding signal profiles assuming that $\langle\sigma v\rangle = 0.5 \times 10^{-26}$ cm^3 s^{-1}. The allowed signal slope becomes much steeper since smaller cross-sections require larger DM densities towards the GC. *We find that there would be significant tension between measured and observationally allowed signal morphologies, both towards the Galactic center ($\psi \lesssim 5^\circ$), but even more importantly in the higher-latitude tail (above $\psi \gtrsim 5^\circ$).*

To enforce consistency between the measured and gravitationally allowed signal morphologies even when dSph limits further strengthen in the future, one would have to resort to more drastic assumptions, such as a DM profile that considerably flattens within the inner 1 kpc or so, or substructure enhancement at larger distances from the GC (which however already seems unlikely to be relevant since due to tidal disruption this effect is expected to be small at $\psi \lesssim 25^\circ$ [126]), or more complex theories of particle DM [127]. We leave the exploration of these scenarios to future work.

Finally, we will estimate the general uncertainty of the annihilation cross-section that is quoted in Tab. I. To this end, we again make use of the above set of valid DM halo models, compatible with the constraints discussed in Ref. [106] at 95% CL. Using all these models, with the additional constraint that $\gamma \geq 1.1$, we find that the line-of-sight integral over the DM density in direction $\psi = 5^\circ$ can vary by a factor 5.9 up and by a factor 0.19 down w.r.t. the value that is obtained for our reference profile ($\gamma = 1.26$, $r_s = 20$ kpc, $\rho_\odot = 0.4$ GeV cm^{-3}). Hence, we attribute a generous astrophysical uncertainty to our best-fit annihilation cross-sections that is multiplicative and in the range $\mathcal{A} = [0.17, 5.3]$. Note that some of the halo models would at face value be too steep in the inner kpc to be compatible with the *Fermi* GeV excess morphology; in these cases we assume that the profile flattens out towards the center.

VI. CONCLUSIONS

In this paper, we presented a critical reassessment of DM interpretations of the *Fermi* GeV excess in light of the foreground/background uncertainties. To this end, we made use of the results from Ref. [26], where the emission from the inner ~ 1 kpc around the GC as seen at higher latitudes ($|b| > 2^\circ$) was robustly characterized with respect to foreground/background uncertainties. In Sec. II, we showed that at the peak energy of 2 GeV, all previous studies of the *Fermi* GeV excess (including the preliminary results from the *Fermi*-LAT team [17]) suggest a signal morphology that is consistent with a contracted DM profile. We entertained here the exciting and suggestive possibility that all of this emission is due to a signal from DM annihilation. Given the complexity of the Galactic foregrounds/backgrounds, we found that a much larger number of DM models fits the gamma-ray data than was previously noted, which should be taken into account in future DM searches. In particular the low- and high- *tails* of the excess energy spectrum, which are highly relevant to constrain different DM scenarios, are subject to large uncertainties.

Our main findings are as follows.

(i) We confirmed previous findings that annihilation to gluons, and quark final states $\bar{q}q$, $\bar{c}c$ and $\bar{b}b$, provide a good fit. However, we found that somewhat higher masses are preferred compared to previous analyses, which is due to the additional uncertainty in the high-energy tail of the energy spectrum. In the case of DM annihilation into $\bar{b}b$, we found that DM masses up to $m_\chi \simeq 74$ GeV are allowed (giving a p-value above 0.05).

(ii) Pure annihilation to pairs of W and Z gauge bosons are excluded at a little over 95% CL. However – and perhaps surprisingly – annihilation to pairs of on shell Higgs bosons produce a rather good fit. Associated gamma-ray lines from $h \to \gamma\gamma$ are close to the sensitivity of current instruments.

(iii) For annihilation into $\mu^+\mu^-$, the ICS emission plays an important role. We showed that it is possible to find CR propagation models for which fits with the ICS emission from $\mu^+\mu^-$ final states and $m_\chi \sim 60$–70 GeV can become competitive with those of annihilation to $\bar{b}b$. Furthermore, we demonstrated that for some models the morphological properties of the GeV excess are well reproduced, and thus that it is not possible to exclude ICS emission from muons only on the basis of gamma-ray data at $|b| > 2^\circ$.

(iv) In a realistic model, DM will likely annihilate into a variety of channels with different branching ratios. We remained agnostic to the composition of allowed final states and derived constraints on different final state triples. In the case of $\bar{b}b$, $\bar{c}c$ and $\tau^+\tau^-$ final states, we found that the best-fit point lies close to the ratios predicted for 2HDM, $\bar{b}b : \bar{c}c : \tau^+\tau^- = 0.87 : 0.08 : 0.05$. We also found that BR($\tau^+\tau^-$) can be substantial (up to around 75%) while still providing a good spectral fit. In the case of annihilation into only $\mu^+\mu^-$ and $\tau^+\tau^-$, we saw that a good fit can always be obtained when BR($\mu^+\mu^-$) $\gtrsim 0.6$ and $m_\chi \sim 50$ GeV. When allowing for additional annihilation into $\bar{q}q$ or $\bar{b}b$, we found that all values of BR($\mu^+\mu^-$) result in a good fit. Lastly, for the annihilation into hh, we found

channel or the DM mass, since we are comparing predicted and measured intensities at the peak of the GeV excess at 2 GeV, which have to be very similar for *any* DM interpretation of the *Fermi* GeV excess.

that a good fit is obtained only when $\mathrm{BR}(hh) \gtrsim 0.8$ and when the DM mass is close to m_h.

(v) For hidden sector models with a light mediator ϕ that subsequently decays into combinations of e^+e^-, $\mu^+\mu^-$ and $\pi^+\pi^-$ – much like in the case of direct annihilation to $\mu^+\mu^-$ – the ICS emission dominates. We found that the allowed DM particle mass range is between 45 and 125 GeV, with cross-sections that are constrained (but not severely) by the AMS positron fraction data.

(vi) We showed that, given dynamical and microlensing constraints on the DM halo, *current limits from dwarf Spheroidal galaxies* are not yet in tension with the DM interpretation of the *Fermi* GeV excess. However, we also demonstrated that if these limits further strengthen by a factor of three, there would be significant tension between measured and observationally allowed *morphologies* of the GC signal. We furthermore showed that given current constraints, the annihilation cross-section is uncertain by a factor of about five up and down (at 95% CL).

The covariance matrix as well as the flux of the *Fermi* GeV excess emission that are used for the spectral analysis are available online.[12]

ACKNOWLEDGMENTS

We thank Markus Ackermann, Carmelo Evoli, Dan Hooper, Gudlaugur Jóhannesson, Simona Murgia, Troy Porter and Neal Weiner for useful discussions. The research of C. W. is part of the VIDI research programme "Probing the Genesis of Dark Matter", which is financed by the Netherlands Organisation for Scientific Research (NWO). This work has been supported by the US Department of Energy. F. C. and C. M. acknowledge support from the European Research Council through the ERC starting grant WIMPs Kairos, P.I. G. Bertone.

Note added. While finalizing this work, a preprint appeared [128] that also considers quarks and massive gauge boson final states in light of the background model systematics from Ref. [26]. For the cases where our analyses overlap we find agreeing results.

[1] G. Jungman, M. Kamionkowski, and K. Griest, *Supersymmetric dark matter*, *Phys.Rept.* **267** (1996) 195–373, [hep-ph/9506380].

[2] L. Bergstrom, *Non-baryonic dark matter: Observational evidence and detection methods*, *Rept. Prog. Phys.* **63** (2000) 793, [hep-ph/0002126].

[3] G. Bertone, D. Hooper, and J. Silk, *Particle dark matter: Evidence, candidates and constraints*, *Phys.Rept.* **405** (2005) 279–390, [hep-ph/0404175].

[4] T. Bringmann and C. Weniger, *Gamma Ray Signals from Dark Matter: Concepts, Status and Prospects*, *Phys.Dark Univ.* **1** (2012) 194–217, [arXiv:1208.5481].

[5] **H.E.S.S.Collaboration** Collaboration, A. Abramowski *et. al.*, *Search for a Dark Matter annihilation signal from the Galactic Center halo with H.E.S.S*, *Phys.Rev.Lett.* **106** (2011) 161301, [arXiv:1103.3266].

[6] D. Hooper, C. Kelso, and F. S. Queiroz, *Stringent and Robust Constraints on the Dark Matter Annihilation Cross Section From the Region of the Galactic Center*, *Astropart.Phys.* **46** (2013) 55–70, [arXiv:1209.3015].

[7] L. Goodenough and D. Hooper, *Possible Evidence For Dark Matter Annihilation In The Inner Milky Way From The Fermi Gamma Ray Space Telescope*, arXiv:0910.2998.

[8] **Fermi/LAT Collaboration** Collaboration, V. Vitale and A. Morselli, *Indirect Search for Dark Matter from the center of the Milky Way with the Fermi-Large Area Telescope*, arXiv:0912.3828.

[9] D. Hooper and L. Goodenough, *Dark Matter Annihilation in The Galactic Center As Seen by the Fermi Gamma Ray Space Telescope*, *Phys.Lett.* **B697** (2011) 412–428, [arXiv:1010.2752].

[10] D. Hooper and T. Linden, *On The Origin Of The Gamma Rays From The Galactic Center*, *Phys.Rev.* **D84** (2011) 123005, [arXiv:1110.0006].

[11] K. N. Abazajian and M. Kaplinghat, *Detection of a Gamma-Ray Source in the Galactic Center Consistent with Extended Emission from Dark Matter Annihilation and Concentrated Astrophysical Emission*, *Phys.Rev.* **D86** (2012) 083511, [arXiv:1207.6047].

[12] C. Gordon and O. Macias, *Dark Matter and Pulsar Model Constraints from Galactic Center Fermi-LAT Gamma Ray Observations*, *Phys.Rev.* **D88** (2013) 083521, [arXiv:1306.5725].

[13] O. Macias and C. Gordon, *The Contribution of Cosmic Rays Interacting With Molecular Clouds to the Galactic Center Gamma-Ray Excess*, *Phys.Rev.* **D89** (2014) 063515, [arXiv:1312.6671].

[14] K. N. Abazajian, N. Canac, S. Horiuchi, and M. Kaplinghat, *Astrophysical and Dark Matter Interpretations of Extended Gamma Ray Emission from the Galactic Center*, arXiv:1402.4090.

[15] T. Daylan, D. P. Finkbeiner, D. Hooper, T. Linden, S. K. N. Portillo, *et. al.*, *The Characterization of the Gamma-Ray Signal from the Central Milky Way: A Compelling Case for Annihilating Dark Matter*, arXiv:1402.6703.

[16] B. Zhou, Y.-F. Liang, X. Huang, X. Li, Y.-Z. Fan, *et. al.*, *GeV excess in the Milky Way: Depending on Diffuse Galactic gamma ray Emission template?*, arXiv:1406.6948.

[17] S. Murgia, *Observation of the high energy gamma-ray emission towards the Galactic center*, 2014. Talk given

[12] https://staff.fnwi.uva.nl/c.weniger/pages/material/

on Fifth Fermi Symposium, Nagoya, 20-24 October 2014.

[18] P. D. Serpico and G. Zaharijas, *Optimal angular window for observing Dark Matter annihilation from the Galactic Center region: the case of γ^- ray lines*, *Astropart.Phys.* **29** (2008) 380–385, [arXiv:0802.3245].

[19] I. Cholis, G. Dobler, D. P. Finkbeiner, L. Goodenough, T. R. Slatyer, *et. al.*, *The Fermi gamma-ray spectrum of the inner galaxy: Implications for annihilating dark matter*, arXiv:0907.3953.

[20] T. Bringmann, F. Calore, G. Vertongen, and C. Weniger, *On the Relevance of Sharp Gamma-Ray Features for Indirect Dark Matter Searches*, *Phys.Rev.* **D84** (2011) 103525, [arXiv:1106.1874].

[21] C. Weniger, *A Tentative Gamma-Ray Line from Dark Matter Annihilation at the Fermi Large Area Telescope*, *JCAP* **1208** (2012) 007, [arXiv:1204.2797].

[22] E. Nezri, J. Lavalle, and R. Teyssier, *Indirect dark matter searches: towards a consistent top-bottom approach for studying the gamma-ray signals and associated backgrounds*, *Phys.Rev.* **D86** (2012) 063524, [arXiv:1204.4121].

[23] M. Tavakoli, I. Cholis, C. Evoli, and P. Ullio, *Constraints on dark matter annihilations from diffuse gamma-ray emission in the Galaxy*, *JCAP* **1401** (2014) 017, [arXiv:1308.4135].

[24] D. Hooper and T. R. Slatyer, *Two Emission Mechanisms in the Fermi Bubbles: A Possible Signal of Annihilating Dark Matter*, *Phys.Dark Univ.* **2** (2013) 118–138, [arXiv:1302.6589].

[25] W.-C. Huang, A. Urbano, and W. Xue, *Fermi Bubbles under Dark Matter Scrutiny. Part I: Astrophysical Analysis*, arXiv:1307.6862.

[26] F. Calore, I. Cholis, and C. Weniger, *Background model systematics for the Fermi GeV excess*, arXiv:1409.0042.

[27] **Fermi-LAT Collaboration** Collaboration, *Fermi-LAT Observations of the Diffuse Gamma-Ray Emission: Implications for Cosmic Rays and the Interstellar Medium*, *Astrophys.J.* **750** (2012) 3, [arXiv:1202.4039].

[28] D. Hooper, I. Cholis, T. Linden, J. Siegal-Gaskins, and T. Slatyer, *Millisecond pulsars Cannot Account for the Inner Galaxy's GeV Excess*, *Phys.Rev.* **D88** (2013) 083009, [arXiv:1305.0830].

[29] F. Calore, M. Di Mauro, and F. Donato, *Diffuse gamma-ray emission from galactic pulsars*, *Astrophys.J.* **796** (2014) 1, [arXiv:1406.2706].

[30] I. Cholis, D. Hooper, and T. Linden, *Challenges in Explaining the Galactic Center Gamma-Ray Excess with Millisecond Pulsars*, arXiv:1407.5625.

[31] J. Petrovic, P. D. Serpico, and G. Zaharijas, *Millisecond pulsars and the Galactic Center gamma-ray excess: the importance of luminosity function and secondary emission*, arXiv:1411.2980.

[32] E. Carlson and S. Profumo, *Cosmic Ray Protons in the Inner Galaxy and the Galactic Center Gamma-Ray Excess*, *Phys.Rev.* **D90** (2014) 023015, [arXiv:1405.7685].

[33] J. Petrovic, P. D. Serpico, and G. Zaharijas, *Galactic Center gamma-ray "excess" from an active past of the Galactic Centre?*, *JCAP* **1410** (2014), no. 10 052, [arXiv:1405.7928].

[34] H. E. Logan, *Dark matter annihilation through a lepton-specific Higgs boson*, *Phys.Rev.* **D83** (2011) 035022, [arXiv:1010.4214].

[35] M. R. Buckley, D. Hooper, and T. M. Tait, *Particle Physics Implications for CoGeNT, DAMA, and Fermi*, *Phys.Lett.* **B702** (2011) 216–219, [arXiv:1011.1499].

[36] G. Zhu, *WIMPless dark matter and the excess gamma rays from the Galactic center*, *Phys.Rev.* **D83** (2011) 076011, [arXiv:1101.4387].

[37] G. Marshall and R. Primulando, *The Galactic Center Region Gamma Ray Excess from A Supersymmetric Leptophilic Higgs Model*, *JHEP* **1105** (2011) 026, [arXiv:1102.0492].

[38] M. Boucenna and S. Profumo, *Direct and Indirect Singlet Scalar Dark Matter Detection in the Lepton-Specific two-Higgs-doublet Model*, *Phys.Rev.* **D84** (2011) 055011, [arXiv:1106.3368].

[39] M. R. Buckley, D. Hooper, and J. L. Rosner, *A Leptophobic Z' And Dark Matter From Grand Unification*, *Phys.Lett.* **B703** (2011) 343–347, [arXiv:1106.3583].

[40] L. A. Anchordoqui and B. J. Vlcek, *W-WIMP Annihilation as a Source of the Fermi Bubbles*, *Phys.Rev.* **D88** (2013) 043513, [arXiv:1305.4625].

[41] M. R. Buckley, D. Hooper, and J. Kumar, *Phenomenology of Dirac Neutralino Dark Matter*, *Phys.Rev.* **D88** (2013) 063532, [arXiv:1307.3561].

[42] K. Hagiwara, S. Mukhopadhyay, and J. Nakamura, *10 GeV neutralino dark matter and light stau in the MSSM*, *Phys.Rev.* **D89** (2014) 015023, [arXiv:1308.6738].

[43] N. Okada and O. Seto, *Gamma ray emission in Fermi bubbles and Higgs portal dark matter*, *Phys.Rev.* **D89** (2014) 043525, [arXiv:1310.5991].

[44] W.-C. Huang, A. Urbano, and W. Xue, *Fermi Bubbles under Dark Matter Scrutiny Part II: Particle Physics Analysis*, *JCAP* **1404** (2014) 020, [arXiv:1310.7609].

[45] K. P. Modak, D. Majumdar, and S. Rakshit, *A Possible Explanation of Low Energy γ-ray Excess from Galactic Centre and Fermi Bubble by a Dark Matter Model with Two Real Scalars*, arXiv:1312.7488.

[46] C. Boehm, M. J. Dolan, C. McCabe, M. Spannowsky, and C. J. Wallace, *Extended gamma-ray emission from Coy Dark Matter*, *JCAP* **1405** (2014) 009, [arXiv:1401.6458].

[47] A. Alves, S. Profumo, F. S. Queiroz, and W. Shepherd, *The Effective Hooperon*, arXiv:1403.5027.

[48] A. Berlin, D. Hooper, and S. D. McDermott, *Simplified Dark Matter Models for the Galactic Center Gamma-Ray Excess*, *Phys.Rev.* **D89** (2014) 115022, [arXiv:1404.0022].

[49] P. Agrawal, B. Batell, D. Hooper, and T. Lin, *Flavored Dark Matter and the Galactic Center Gamma-Ray Excess*, *Phys.Rev.* **D90** (2014) 063512, [arXiv:1404.1373].

[50] E. Izaguirre, G. Krnjaic, and B. Shuve, *The Galactic Center Excess from the Bottom Up*, *Phys.Rev.* **D90** (2014) 055002, [arXiv:1404.2018].

[51] D. Cerden, M. Peiro, and S. Robles, *Low-mass right-handed sneutrino dark matter: SuperCDMS and LUX constraints and the Galactic Centre gamma-ray excess*, *JCAP* **1408** (2014) 005, [arXiv:1404.2572].

[52] S. Ipek, D. McKeen, and A. E. Nelson, *A Renormalizable Model for the Galactic Center Gamma*

Ray Excess from Dark Matter Annihilation, *Phys.Rev.* **D90** (2014) 055021, [arXiv:1404.3716].

[53] C. Boehm, M. J. Dolan, and C. McCabe, *A weighty interpretation of the Galactic Centre excess*, *Phys.Rev.* **D90** (2014) 023531, [arXiv:1404.4977].

[54] P. Ko, W.-I. Park, and Y. Tang, *Higgs portal vector dark matter for* GeV *scale γ-ray excess from galactic center*, *JCAP* **1409** (2014) 013, [arXiv:1404.5257].

[55] M. Abdullah, A. DiFranzo, A. Rajaraman, T. M. Tait, P. Tanedo, *et. al.*, *Hidden On-Shell Mediators for the Galactic Center Gamma-Ray Excess*, *Phys.Rev.* **D90** (2014) 035004, [arXiv:1404.6528].

[56] D. K. Ghosh, S. Mondal, and I. Saha, *Confronting the Galactic Center Gamma Ray Excess With a Light Scalar Dark Matter*, arXiv:1405.0206.

[57] A. Martin, J. Shelton, and J. Unwin, *Fitting the Galactic Center Gamma-Ray Excess with Cascade Annihilations*, arXiv:1405.0272.

[58] T. Basak and T. Mondal, *Class of Higgs-portal Dark Matter models in the light of gamma-ray excess from Galactic center*, arXiv:1405.4877.

[59] A. Berlin, P. Gratia, D. Hooper, and S. D. McDermott, *Hidden Sector Dark Matter Models for the Galactic Center Gamma-Ray Excess*, *Phys.Rev.* **D90** (2014) 015032, [arXiv:1405.5204].

[60] J. M. Cline, G. Dupuis, Z. Liu, and W. Xue, *The windows for kinetically mixed Z'-mediated dark matter and the galactic center gamma ray excess*, *JHEP* **1408** (2014) 131, [arXiv:1405.7691].

[61] T. Han, Z. Liu, and S. Su, *Light Neutralino Dark Matter: Direct/Indirect Detection and Collider Searches*, *JHEP* **1408** (2014) 093, [arXiv:1406.1181].

[62] W. Detmold, M. McCullough, and A. Pochinsky, *Dark Nuclei I: Cosmology and Indirect Detection*, arXiv:1406.2276.

[63] L. Wang, *A simplified 2HDM with a scalar dark matter and the galactic center gamma-ray excess*, arXiv:1406.3598.

[64] W.-F. Chang and J. N. Ng, *A Minimal Model of Majoronic Dark Radiation and Dark Matter*, *Phys.Rev.* **D90** (2014) 065034, [arXiv:1406.4601].

[65] C. Arina, E. Del Nobile, and P. Panci, *Not so Coy Dark Matter explains DAMA (and the Galactic Center excess)*, arXiv:1406.5542.

[66] C. Cheung, M. Papucci, D. Sanford, N. R. Shah, and K. M. Zurek, *NMSSM Interpretation of the Galactic Center Excess*, *Phys.Rev.* **D90** (2014) 075011, [arXiv:1406.6372].

[67] S. D. McDermott, *Lining up the Galactic Center Gamma-Ray Excess*, arXiv:1406.6408.

[68] J. Huang, T. Liu, L.-T. Wang, and F. Yu, *Supersymmetric Sub-Electroweak Scale Dark Matter, the Galactic Center Gamma-ray Excess, and Exotic Decays of the 125 GeV Higgs Boson*, arXiv:1407.0038.

[69] C. Balazs and T. Li, *Simplified Dark Matter Models Confront the Gamma Ray Excess*, *Phys.Rev.* **D90** (2014) 055026, [arXiv:1407.0174].

[70] P. Ko and Y. Tang, *Galactic center γ-ray excess in hidden sector DM models with dark gauge symmetries: local Z_3 symmetry as an example*, arXiv:1407.5492.

[71] N. Okada and O. Seto, *Galactic center gamma ray excess from two Higgs doublet portal dark matter*, *Phys.Rev.* **D90** (2014), no. 8 083523, [arXiv:1408.2583].

[72] K. Ghorbani, *Fermionic dark matter with pseudo-scalar Yukawa interaction*, arXiv:1408.4929.

[73] A. D. Banik and D. Majumdar, *Low Energy Gamma Ray Excess Confronting a Singlet Scalar Extended Inert Doublet Dark Matter Model*, arXiv:1408.5795.

[74] D. Borah and A. Dasgupta, *Galactic Center Gamma Ray Excess in a Radiative Neutrino Mass Model*, arXiv:1409.1406.

[75] M. Cahill-Rowley, J. Gainer, J. Hewett, and T. Rizzo, *Towards a Supersymmetric Description of the Fermi Galactic Center Excess*, arXiv:1409.1573.

[76] J. Guo, J. Li, T. Li, and A. G. Williams, *NMSSM Explanations of the Galactic Gamma Ray Excess and Promising LHC Searches*, arXiv:1409.7864.

[77] M. Freytsis, D. J. Robinson, and Y. Tsai, *Galactic Center Gamma-Ray Excess through a Dark Shower*, arXiv:1410.3818.

[78] M. Heikinheimo and C. Spethmann, *Galactic Centre GeV Photons from Dark Technicolor*, *JHEP* **1412** (2014) 084, [arXiv:1410.4842].

[79] G. Arcadi, Y. Mambrini, and F. Richard, *Z-portal dark matter*, arXiv:1411.2985.

[80] F. Richard, G. Arcadi, and Y. Mambrini, *Search for Dark Matter at Colliders*, arXiv:1411.0088.

[81] N. F. Bell, S. Horiuchi, and I. M. Shoemaker, *Annihilating Asymmetric Dark Matter*, *Phys.Rev.* **D91** (2015) 023505, [arXiv:1408.5142].

[82] L. Bergstrom, T. Bringmann, I. Cholis, D. Hooper, and C. Weniger, *New limits on dark matter annihilation from AMS cosmic ray positron data*, *Phys.Rev.Lett.* **111** (2013) 171101, [arXiv:1306.3983].

[83] A. Ibarra, A. S. Lamperstorfer, and J. Silk, *Dark matter annihilations and decays after the AMS-02 positron measurements*, *Phys.Rev.* **D89** (2014) 063539, [arXiv:1309.2570].

[84] T. Bringmann, M. Vollmann, and C. Weniger, *Updated cosmic-ray and radio constraints on light dark matter: Implications for the GeV gamma-ray excess at the Galactic center*, arXiv:1406.6027.

[85] M. Cirelli, D. Gaggero, G. Giesen, M. Taoso, and A. Urbano, *Antiproton constraints on the GeV gamma-ray excess: a comprehensive analysis*, arXiv:1407.2173.

[86] C. Evoli, I. Cholis, D. Grasso, L. Maccione, and P. Ullio, *Antiprotons from dark matter annihilation in the Galaxy: astrophysical uncertainties*, *Phys.Rev.* **D85** (2012) 123511, [arXiv:1108.0664].

[87] I. Cholis, *New Constraints from PAMELA anti-proton data on Annihilating and Decaying Dark Matter*, *JCAP* **1109** (2011) 007, [arXiv:1007.1160].

[88] F. Donato, D. Maurin, P. Brun, T. Delahaye, and P. Salati, *Constraints on WIMP Dark Matter from the High Energy PAMELA $\bar{p}/p$ data*, *Phys. Rev. Lett.* **102** (2009) 071301, [arXiv:0810.5292].

[89] R. Kappl and M. W. Winkler, *Dark Matter after BESS-Polar II*, *Phys.Rev.* **D85** (2012) 123522, [arXiv:1110.4376].

[90] D. Hooper, T. Linden, and P. Mertsch, *What Does The PAMELA Antiproton Spectrum Tell Us About Dark Matter?*, arXiv:1410.1527.

[91] A. Geringer-Sameth, S. M. Koushiappas, and M. G. Walker, *A Comprehensive Search for Dark Matter Annihilation in Dwarf Galaxies*, arXiv:1410.2242.

[92] I. Cholis and P. Salucci, *Extracting limits on Dark Matter annihilation from gamma-ray observations towards dwarf spheroidal galaxies*, *Phys.Rev.* **D86** (2012) 023528, [arXiv:1203.2954].

[93] A. Geringer-Sameth and S. M. Koushiappas, *Exclusion of canonical WIMPs by the joint analysis of Milky Way dwarfs with Fermi*, *Phys.Rev.Lett.* **107** (2011) 241303, [arXiv:1108.2914].

[94] **Fermi-LAT Collaboration** Collaboration, A. Abdo *et. al.*, *Observations of Milky Way Dwarf Spheroidal galaxies with the Fermi-LAT detector and constraints on Dark Matter models*, *Astrophys.J.* **712** (2010) 147–158, [arXiv:1001.4531].

[95] R. Catena and P. Ullio, *A novel determination of the local dark matter density*, *JCAP* **1008** (2010) 004, [arXiv:0907.0018].

[96] P. Salucci, F. Nesti, G. Gentile, and C. Martins, *The dark matter density at the Sun's location*, *Astron.Astrophys.* **523** (2010) A83, [arXiv:1003.3101].

[97] P. Gondolo, J. Edsjo, P. Ullio, L. Bergstrom, M. Schelke, *et. al.*, *DarkSUSY: Computing supersymmetric dark matter properties numerically*, *JCAP* **0407** (2004) 008, [astro-ph/0406204].

[98] T. Sjostrand, S. Mrenna, and P. Z. Skands, *PYTHIA 6.4 Physics and Manual*, *JHEP* **0605** (2006) 026, [hep-ph/0603175].

[99] M. Cirelli, G. Corcella, A. Hektor, G. Hutsi, M. Kadastik, *et. al.*, *PPPC 4 DM ID: A Poor Particle Physicist Cookbook for Dark Matter Indirect Detection*, *JCAP* **1103** (2011) 051, [arXiv:1012.4515].

[100] T. Sjostrand, S. Mrenna, and P. Z. Skands, *A Brief Introduction to PYTHIA 8.1*, *Comput.Phys.Commun.* **178** (2008) 852–867, [arXiv:0710.3820].

[101] **Particle Data Group** Collaboration, K. Olive *et. al.*, *Review of Particle Physics*, *Chin.Phys.* **C38** (2014) 090001.

[102] C. Jackson, G. Servant, G. Shaughnessy, T. M. Tait, and M. Taoso, *Higgs in Space!*, *JCAP* **1004** (2010) 004, [arXiv:0912.0004].

[103] N. Bernal, C. Boehm, S. Palomares-Ruiz, J. Silk, and T. Toma, *Observing Higgs boson production through its decay into gamma-rays: A messenger for Dark Matter candidates*, *Phys.Lett.* **B723** (2013) 100–106, [arXiv:1211.2639].

[104] **Fermi-LAT Collaboration** Collaboration, M. Ackermann *et. al.*, *Search for Gamma-ray Spectral Lines with the Fermi Large Area Telescope and Dark Matter Implications*, *Phys.Rev.* **D88** (2013) 082002, [arXiv:1305.5597].

[105] A. Ibarra, S. Lopez Gehler, and M. Pato, *Dark matter constraints from box-shaped gamma-ray features*, *JCAP* **1207** (2012) 043, [arXiv:1205.0007].

[106] F. Iocco, M. Pato, G. Bertone, and P. Jetzer, *Dark Matter distribution in the Milky Way: microlensing and dynamical constraints*, *JCAP* **1111** (2011) 029, [arXiv:1107.5810].

[107] T. Lacroix, C. Boehm, and J. Silk, *Fitting the Fermi-LAT GeV excess: On the importance of including the propagation of electrons from dark matter*, *Phys.Rev.* **D90** (2014) 043508, [arXiv:1403.1987].

[108] A. W. Strong and I. V. Moskalenko, *Propagation of cosmic-ray nucleons in the Galaxy*, *Astrophys. J.* **509** (1998) 212–228, [astro-ph/9807150].

[109] A. W. Strong, I. V. Moskalenko, T. A. Porter, E. Orlando, S. W. Diger, and A. E. Vladimirov, *GALPROP Version 54: Explanatory Supplement*, 2011.

[110] C. Boehm *et. al. Work in progress.*

[111] B. Patt and F. Wilczek, *Higgs-field portal into hidden sectors*, hep-ph/0605188.

[112] G. D'Ambrosio, G. Giudice, G. Isidori, and A. Strumia, *Minimal flavor violation: An Effective field theory approach*, *Nucl.Phys.* **B645** (2002) 155–187, [hep-ph/0207036].

[113] V. Silveira and A. Zee, *Scalar Phantoms*, *Phys.Lett.* **B161** (1985) 136.

[114] J. McDonald, *Gauge singlet scalars as cold dark matter*, *Phys.Rev.* **D50** (1994) 3637–3649, [hep-ph/0702143].

[115] C. Burgess, M. Pospelov, and T. ter Veldhuis, *The Minimal model of nonbaryonic dark matter: A Singlet scalar*, *Nucl.Phys.* **B619** (2001) 709–728, [hep-ph/0011335].

[116] J. M. Cline, K. Kainulainen, P. Scott, and C. Weniger, *Update on scalar singlet dark matter*, *Phys.Rev.* **D88** (2013) 055025, [arXiv:1306.4710].

[117] D. P. Finkbeiner and N. Weiner, *Exciting Dark Matter and the INTEGRAL/SPI 511 keV signal*, *Phys.Rev.* **D76** (2007) 083519, [astro-ph/0702587].

[118] N. Arkani-Hamed, D. P. Finkbeiner, T. R. Slatyer, and N. Weiner, *A Theory of Dark Matter*, *Phys.Rev.* **D79** (2009) 015014, [arXiv:0810.0713].

[119] D. Hooper, N. Weiner, and W. Xue, *Dark Forces and Light Dark Matter*, *Phys.Rev.* **D86** (2012) 056009, [arXiv:1206.2929].

[120] I. Cholis, D. P. Finkbeiner, L. Goodenough, and N. Weiner, *The PAMELA Positron Excess from Annihilations into a Light Boson*, *JCAP* **0912** (2009) 007, [arXiv:0810.5344].

[121] I. Cholis, G. Dobler, D. P. Finkbeiner, L. Goodenough, and N. Weiner, *The Case for a 700+ GeV WIMP: Cosmic Ray Spectra from ATIC and PAMELA*, *Phys.Rev.* **D80** (2009) 123518, [arXiv:0811.3641].

[122] J. Liu, N. Weiner, and W. Xue, *Signals of a Light Dark Force in the Galactic Center*, arXiv:1412.1485.

[123] D. P. Finkbeiner, L. Goodenough, T. R. Slatyer, M. Vogelsberger, and N. Weiner, *Consistent Scenarios for Cosmic-Ray Excesses from Sommerfeld-Enhanced Dark Matter Annihilation*, *JCAP* **1105** (2011) 002, [arXiv:1011.3082].

[124] B. Anderson, *A Search for Dark Matter Annihilation in Dwarf Spheroidal Galaxies with Pass 8 Data*, 2014. Talk given on Fifth Fermi Symposium, Nagoya, 20-24 October 2014.

[125] M. Wood, *New Fermi-LAT Results on the Search for Dark Matter Annihilation in Dwarf Spheroidal Galaxies*, 2014. SLAC Experimental Physics Seminar, 14 October 2014.

[126] L. Pieri, J. Lavalle, G. Bertone, and E. Branchini, *Implications of High-Resolution Simulations on Indirect Dark Matter Searches*, *Phys.Rev.* **D83** (2011) 023518, [arXiv:0908.0195].

[127] E. Hardy, R. Lasenby, and J. Unwin, *Annihilation Signals from Asymmetric Dark Matter*, *JHEP* **1407** (2014) 049, [arXiv:1402.4500].

[128] P. Agrawal, B. Batell, P. J. Fox, and R. Harnik, *WIMPs at the Galactic Center*, arXiv:1411.2592.